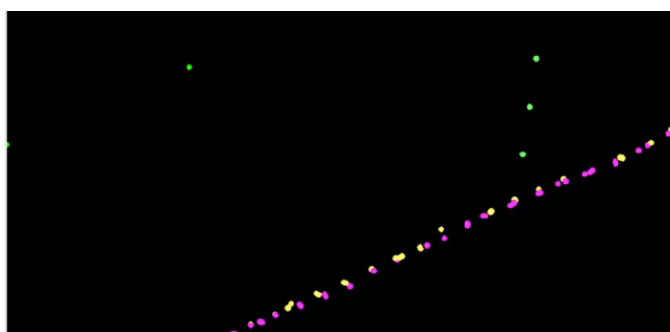
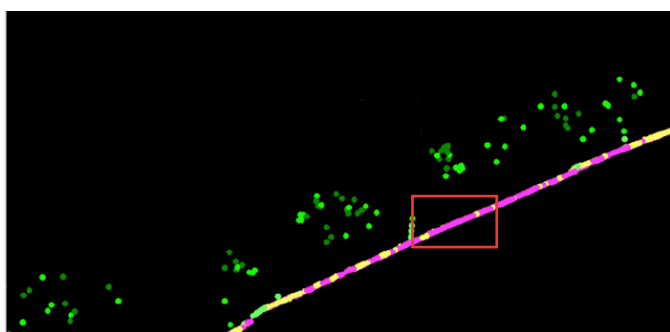
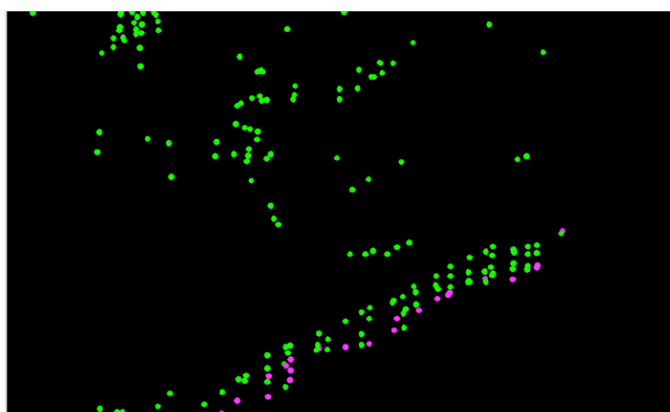
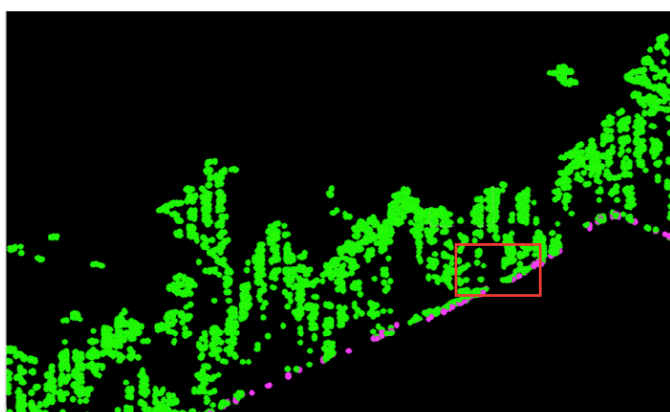


PROJECT SUMMARY:

Western Tasmania Geoscience Initiative

Luina LiDAR Survey

by David C. Green





Mineral Resources Tasmania

PO Box 56

Rosny Park Tasmania 7018

Phone (03) 6165 4800

Fax (03) 62338338

Email info@mrt.tas.gov.au

Internet www.mrt.tas.gov.au

December 2017

Refer to this document as:

Green, David C. 2017. Western Tasmania Geoscience Initiative Luina LiDAR Survey. Tasmanian Geological Survey Record 2017/04. Mineral Resources Tasmania.

Cover photo:

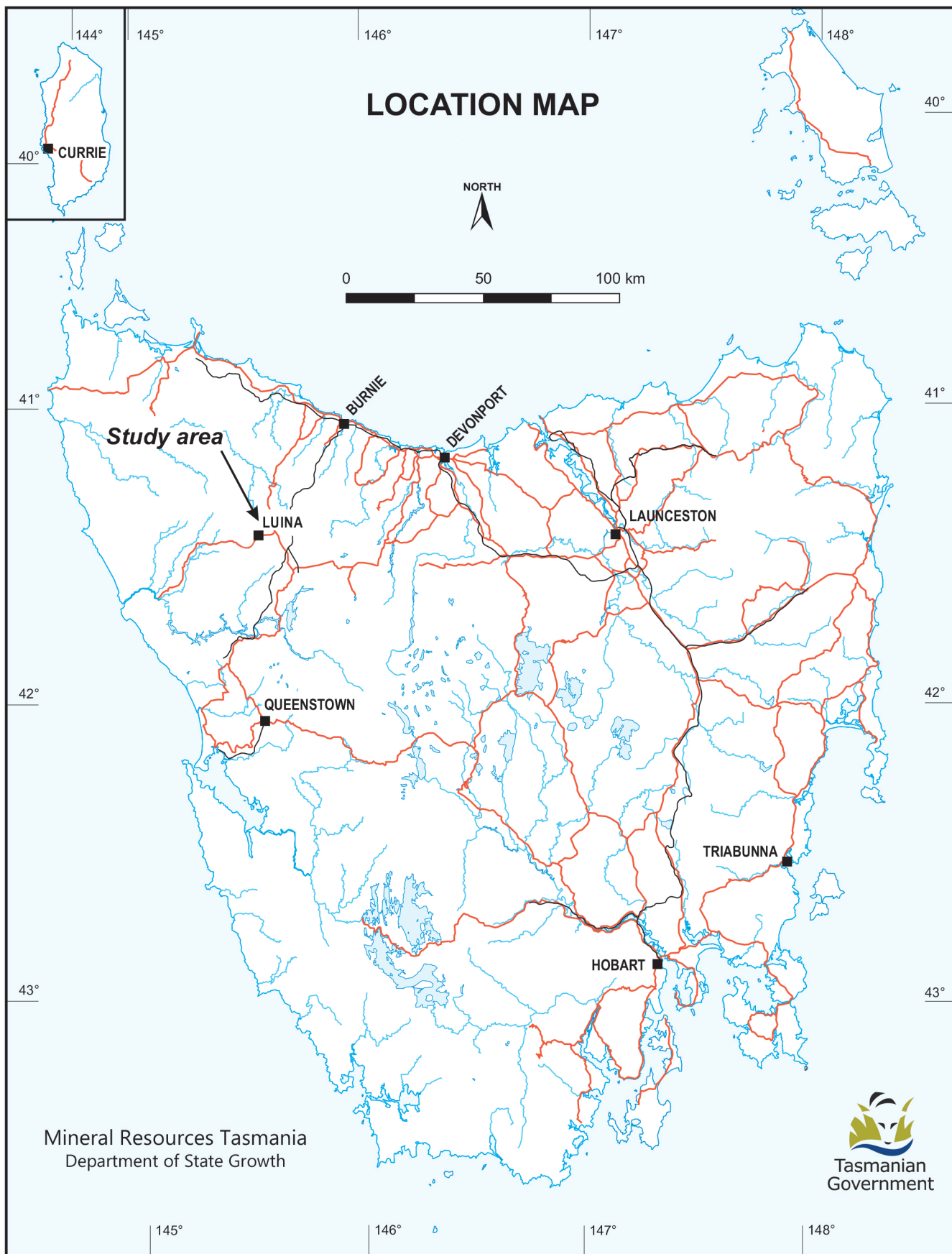
LiDAR point cloud cross sections from Luina and Mathinna illustrating differences in ground point distribution..

While every care has been taken in the preparation of this report, no warranty is given as to the correctness of the information and no liability is accepted for any statement or opinion or for any error or omission. No reader should act or fail to act on the basis of any material contained herein. Readers should consult professional advisers. As a result the Crown in Right of the State of Tasmania and its employees, contractors and agents expressly disclaim all and any liability (including all liability from or attributable to any negligent or wrongful act or omission) to any persons whatsoever in respect of anything done or omitted to be done by any such person in reliance whether in whole or in part upon any of the material in this report.

Tasmanian Geological Survey Record UR2017/04

PROJECT SUMMARY:
Western Tasmania Geoscience Initiative Luina LiDAR survey

by David C. Green



CONTENTS

Abstract	7
Introduction	7
The LiDAR method in forested terrains	8
Experiment design	10
Regional survey results	12
Experiment results and discussion	13
Off nadir	13
Spot specification	18
Filling in the gaps	20
Effect of ground cover	28
Conclusions	28
References	29
Appendix 1 The effect of spot size and off-nadir angle	31
Appendix 2 AAM proposal	33
Appendix 3 Survey specifications	41
Appendix 4 AAM survey acquisition report	45
Appendix 5 Spline interpolation	55
Appendix 6 DEM interpolation processing logs	59
Appendix 7 MOI tools	63

List of figures

Figure 1	The location of the Luina LiDAR survey.....	8
Figure 2	The vegetation of the survey area	9
Figure 3	The range of LiDAR pulse specifications available for the Optech Pegasus	11
Figure 4	This hillshaded DEM of the Magnet mine area	14
Figure 5	The Luina Group characterised by simple curvi-linear bedding traces in the centre of the image	15
Figure 6	The Luina Group in the northern part of Mt Cleveland.....	16
Figure 7	Detail in the Oonah Formation	17
Figure 8	The relationship between off-nadir angle and number of ground returns.....	18
Figure 9	The experimental spot specification space contoured by proportion of emitted pulses returned from the ground	19
Figure 10	The effect of spot size on forest penetration	21
Figure 11	The experimental spot specification space contoured by cost per ground point	22
Figure 12	Top: Cross section of the LiDAR point cloud in typical forested terrain Bottom: ground point density	23
Figure 13	Histogram of ground points as a function of ground point density	24
Figure 14	Histogram of ground points for areas of low ground point density	24
Figure 15	The experimental spot specification space contoured by cost per thousand ground points.....	25
Figure 16	Hillshaded DEMs interpolated only from ground points under tall trees	26
Figure 17	Hill-shaded DEMs of portions of the Mathinna and Luina LiDAR surveys	27
Figure 18	LiDAR point cloud cross sections from Luina and Mathinna	28
Figure A1.1	Leica's experiment to measure the decrease in forest penetration as off-nadir angle increases	31
Figure A1.2	Leica's experiment to measure the effect of spot size on forest penetration	32
Figure A1.3	The calculated effect of off-nadir angle on the laser spot characteristics	32
Figure A5.1	Spline fits for various lambda	55
Figure A5.2	Smoothing parameter selection for pressure	56
Figure A5.3	A collation of hillshaded DEMs	57

List of tables

Table 1	Experimental parameters	12
Table 2	Leica's experiment to measure the effect of spot size on forest penetration	13
Table 3	Experiment results: Ground point density for off-nadir angle $\leq 12^\circ$	19

ABSTRACT

A LiDAR (Light Detection And Ranging) survey was flown over 100 km² of heavily forested sections of northwestern Tasmania as part of the Western Tasmanian Geoscience Initiative. The aims of the survey were to find the LiDAR survey settings that optimise laser pulse returns from the ground through thick rainforest and to produce a Digital Elevation Model (DEM) to aid geological interpretation.

The survey was processed using a minimum curvature interpolation to produce a 1 m DEM. The DEM is rich in geological information, including bedding traces, folds and built infrastructure. A practical tool was developed by Matthew Cracknell to extract plane orientations from bedding traces in the ArcMap environment.

Four experimental swathes were flown, covering the full range of laser spot parameters available for the LiDAR instrument. The results show that the most cost-effective spot specification for maximising ground points through rainforest is the industry standard setting with a moderate spot size, low power (high pulse rate frequency) and 25° full field of view. The standard survey settings achieved an average ground point spacing of 1.7 m, but areas under tall trees were poorly represented, with 32% of the area returning a point spacing of 7 m. If a large spot diameter was used, it would be possible to achieve a point spacing under tall trees of at best 3.3 m and would cost 2.5 times that of a standard survey. Further reduction of point spacing would require multiple swathes.

Note: All coordinates are MGA and use the GDA94 datum.

INTRODUCTION

Gaps in our geological knowledge of the west coast of Tasmania are in large part due to the inaccessibility of large areas. Remote sensing methods have provided datasets useful in producing interpretive maps for field checking but are less useful in areas that lack rocks with contrasting geophysical

properties. It was demonstrated in the TasExplore Project in northeast Tasmania that LiDAR has the capability of providing a high-resolution DEM rich in geological features from which a geological map can be produced efficiently (Green and Bombardieri, 2013). In this project geological features such as bedding traces could be seen in high-resolution (1–2 m) DEMs. Cracknell (2009) and Cracknell et al. (2013) used a 5 m DEM to extract structural bedding data, which was used to interpret the three-dimensional geology of the Tyne-Mathinna area. Field work to ground truth interpretations and map lithologies led to the efficient production of a new 1:25,000 geological map.

While the use of LiDAR in lightly forested northeast Tasmania proved to be successful, LiDAR surveys in rainforested areas in western Tasmania in 2008–2012, chiefly by mineral exploration companies, produced relatively poor DEMs, characterised by poor ground point density (average point spacing of 5–30 m), high noise and numerous classification errors. The DEMs contained little geological information at high resolution. Advances in LiDAR instrumentation, including increased power, increased pulse frequency, decreased echo separation and faster detection electronics indicate that the technology may now be capable of producing much improved DEMs in rainforested areas.

The aims of the Luina LiDAR survey were to:

- Demonstrate the practicality of obtaining a high-quality LiDAR DEM in rainforested areas.
- Assist in efficiently creating a geological map in an area difficult to access by providing a LiDAR DEM of sufficient resolution to reveal geological information such as stratigraphy, folding and faulting.
- Test a range of LiDAR survey specifications to optimise the canopy penetration of LiDAR pulses and maximise the proportion of pulses returned from the ground.

The Luina survey was completed as part of the Western Tasmanian Geoscience Initiative, and was flown over a 100 km² area underlain by Luina Group and Oonah Formation rocks that was subject to geological mapping as part of the same project (Fig. 1). One north–south line was chosen as a representative target for repeated LiDAR surveys with varying survey specifications.

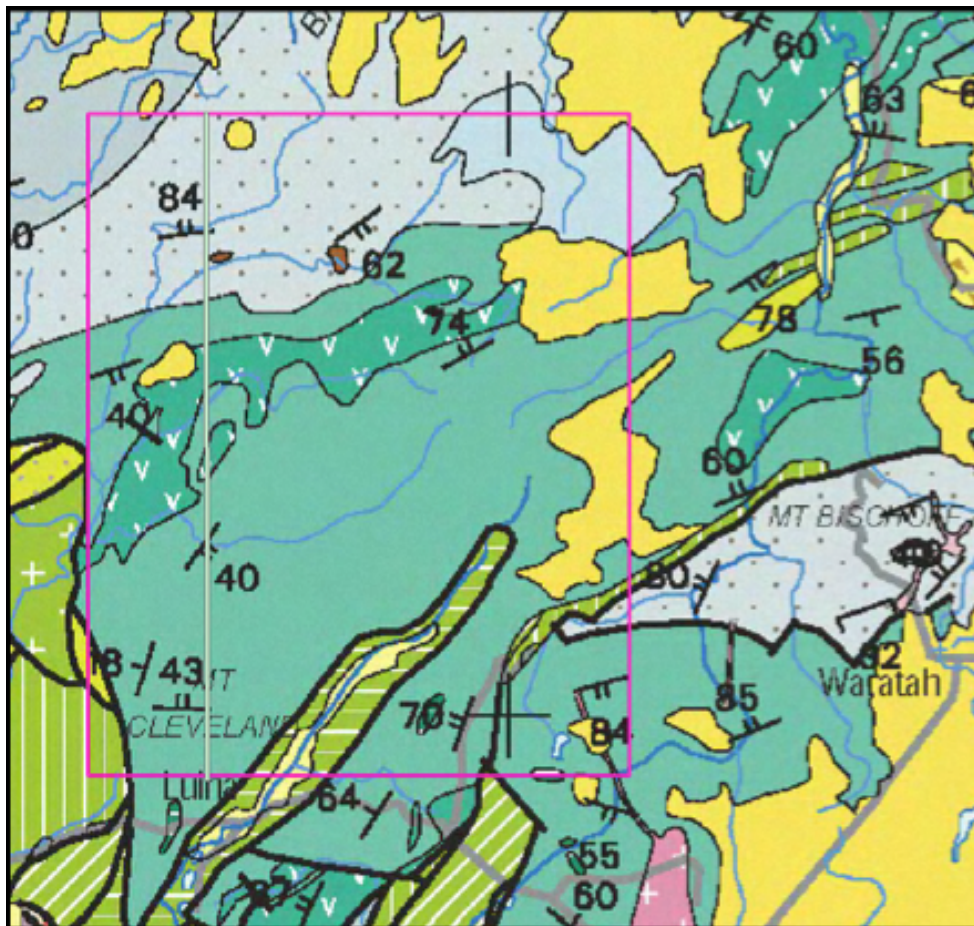


FIGURE 1. The location of the Luina LiDAR survey (10 km x 11 km) is outlined in pink on a 1:250,000 geology coverage. The Oonah Formation is illustrated in grey and the Luina Group in green, with basalt indicated with a 'v' annotation and mafic-ultramafic complexes with horizontal ornament. The repeated LiDAR swath is depicted by the green line oriented north–south through Mt Cleveland.

The Luina survey area has large-scale topographic features oriented generally NNE–SSW to ENE–WSW with a relief of about 200 m with typical slopes of 19°.

The underlying geology is chiefly Luina Group, a probable Early Cambrian volcanosedimentary broken formation in all but the most northwesterly portion, which is underlain by folded more siliceous, turbiditic Neoproterozoic Oonah Formation. The Luina Group is dominated by mudstone/shale, volcanoclastic sandstone and tholeiitic basalt with subordinate chert and carbonate and encloses the Heazlewood River, Whyte River and Magnet mafic-ultramafic complexes. The Oonah formation comprises continent-derived turbidite sequences (mudstone and sandstone) interbedded with minor pillow basalt.

The entire area is heavily vegetated by rainforest with a typical canopy at 30 m and dense under-

growth (Fig. 2). The canopy trees are typically *Nothofagus cunninghamii* (southern beech) with emergent *Eucalyptus obliqua* (stringy bark), with a commonly dense and tangled understorey of widely varying small-leaved trees including *Anodopetalum*, *Telopea* and *Leptospermum* species. The undergrowth is dominated by ground ferns and broad leaf shrubs.

The LiDAR method in forested terrains

LiDAR consists of a pulsed laser ranging system mounted in an aircraft equipped with a precise kinematic GPS receiver and an inertial navigation system (Wehr and Lohr, 1999). Each laser pulse sent towards the earth is reflected back towards the aircraft where it is captured. Using a rotating mirror inside the laser transmitter, the laser pulses are made to scan back and forth producing a zig-zag pattern of LiDAR hits along the flight path.

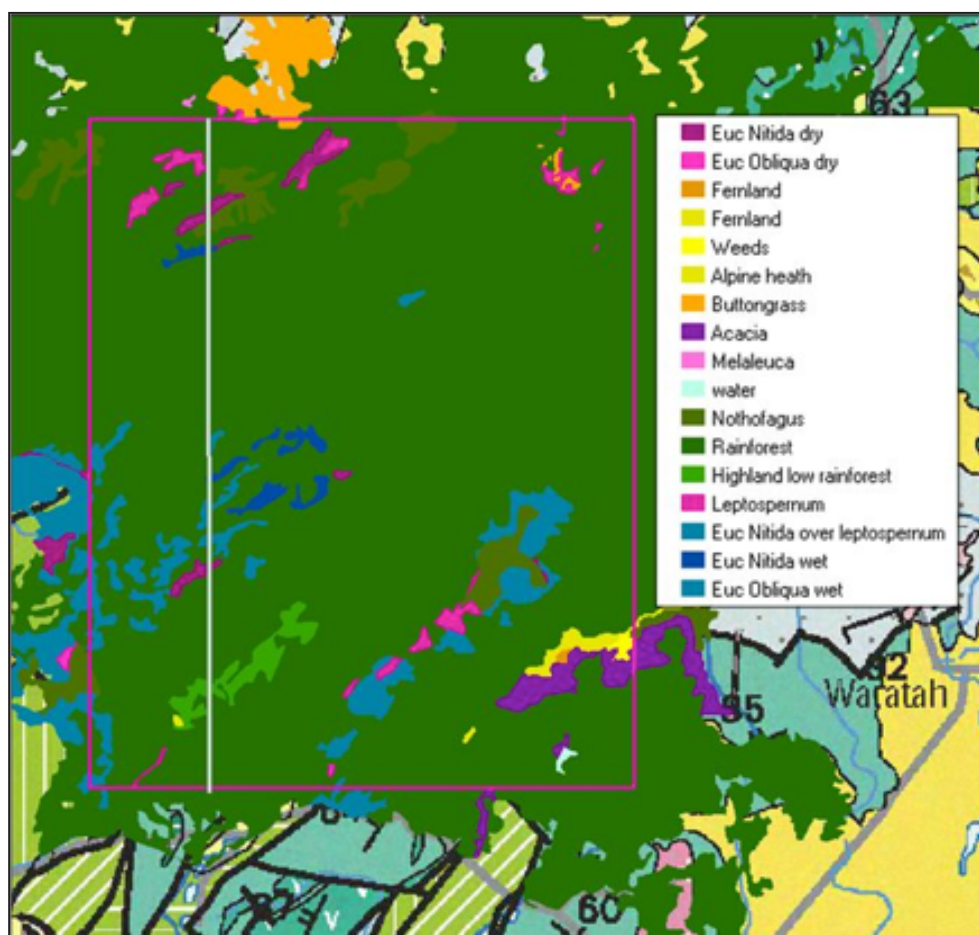


FIGURE 2. The vegetation of the survey area illustrated on a map derived from Figure 1, illustrating vegetation types derived from the Department of Primary Industries, Parks, Water and Environment TasVeg database. The bulk of the surveyed area is classified as rainforest.

Accurately timing pulses gives the distance to the reflecting features. After correcting for the laser and aircraft orientation and GPS position, the location of the reflector can be determined accurately. The located return pulses create a three-dimensional “point cloud” consisting of reflections off a variety of features, which are classified by the service provider into ground and other features. Ground features can be interpolated to produce a DEM under a forested canopy (Nyborg et al., 2007).

In heavily forested areas, it has been found that LiDAR pulses have difficulty in penetrating the canopy with a result that there are not enough near-ground points to confidently classify as ground. The resulting DEMs are characterised by poor resolution, point anomalies due to misclassified returns and noise of a magnitude similar to the expected geological signal (i.e., tens of centimetres). A typical example is the Ringarooma LiDAR DEM,

flown at similar specifications as other areas of northeast Tasmania as part of the TasExplore project in 2008. While other surveys flown over light forest returned high-resolution DEMs rich in geological information, the Ringarooma area was flown over heavily forested terrain and the DEM contained little geological information.

The challenge of producing high-resolution LiDAR DEMs in heavily forested terrain is not a problem unique to Tasmania. Attempts to address the problem have been undertaken by several agencies by massively increasing the density of emitted laser pulses. For example GNS Science New Zealand (Langridge et al., 2014) successfully created a 2 m DEM in the Gaunt Creek region of the Alpine Fault through thick podocarp forest by flying two sets of mutually orthogonal flight lines using standard specifications. Archaeological ruins have been mapped successfully through tropical jungle in

Belize (Chase et al., 2011) by flying relatively low with a high degree of flight line sidelap/overlap.

While these examples demonstrate success simply by sending out more laser pulses, the cost can become excessive. A complementary strategy is to tailor the characteristics of the emitted laser pulse to optimise canopy penetration and maximise returns from the ground, effectively getting more out of each pulse. Australian LiDAR service providers and consultants with experience in Victorian wet eucalypt forest almost ubiquitously recommended relatively small diameter pulses and staying close to nadir. In contrast, Fugro were able to provide experimental data from repeated surveys over maple-oak-ash-birch forest in Massachusetts demonstrating increased canopy penetration for large spot sizes and a significant decline in ground returns when more than 15° off nadir (Leica Geosystems 2009, reproduced in part in Appendix 1).

EXPERIMENT DESIGN

Although previous work in rainforests has been successful in producing high-resolution DEMs through thick forest, strategies have either not been concerned with cost, or have not been used in terrain similar to Tasmanian conditions. The work is therefore not suitable to guide a LiDAR survey specification designed to maximise canopy penetration in western Tasmania. The Luina survey planned to include four experiments to measure the effectiveness of a range of pulse characteristics in penetrating rainforest. This was to be accomplished by repeating one swath several times with different pulse specifications.

A service provider was selected based on demonstrated performance in producing DEMs in areas of thick forest, and their appreciation of the experiments. AAM completed the survey in 2013 using a newly released instrument, the Optech Pegasus HD500, which featured current high performance in pulse rate frequency (500 kHz), narrow spot divergence (0.2 mrad), ground pattern (zig-zag), range capture (4), echo separation (1.0 m) and field of view (70°) (Appendix 2: AAM proposal). Optech also advocated that the

instrument incorporated two LiDAR instruments, one directed 2° forward of the other, promoted by AAM as beneficial for maximising ground returns from forest floors.

The pulse characteristics identified that are likely to directly affect canopy penetration are pulse diameter, laser intensity, off-nadir angle and laser wavelength. The Pegasus allowed experimentation with the pulse intensity and flight planning allowed experimentation with pulse diameter and off-nadir angle. The combined pulse specification can be summarised in a plot of pulse intensity versus pulse diameter. Figure 3 illustrates the experimental space available for the Pegasus instrument, bounded by power availability, laser eye-safety regulations, detector sensitivity and the speed of the electronics and software associated with analysing returns. Pulse intensity near the ground is determined by a combination of pulse rate frequency (PRF), with a lower PRF resulting in more power per pulse, and flying height. As the Pegasus does not have adjustable beam divergence, pulse diameter on the ground was determined solely by flying height.

Four pulse specifications were selected to fill the experimental space and suitable survey designs were proposed by AAM (Appendix 3: Survey specifications). In order to keep the surveys comparable but simple, significant variation in down-track:cross-track point spacing ratio and in emitted pulse density was incurred, ranging from a ratio of 0.55 to 2.02 and a point density of 1.9 to 4.8 points/m². Variations in emitted point density were corrected for when assessing the proportion of emitted pulses returned from the ground.

Hence the experiments planned were:

- Measure the canopy penetration with varying combinations of spot diameter and spot intensity.
- Measure the canopy penetration with varying off-nadir angle.

The most cost-effective survey in terms of emitted pulse density used a low spot intensity and moderate spot diameter, and was achieved using a high PRF and moderate flying height. This type of specification, resulting in a maximally dense point cloud, is generally the preferred option for survey contractors. The Luina experiments used

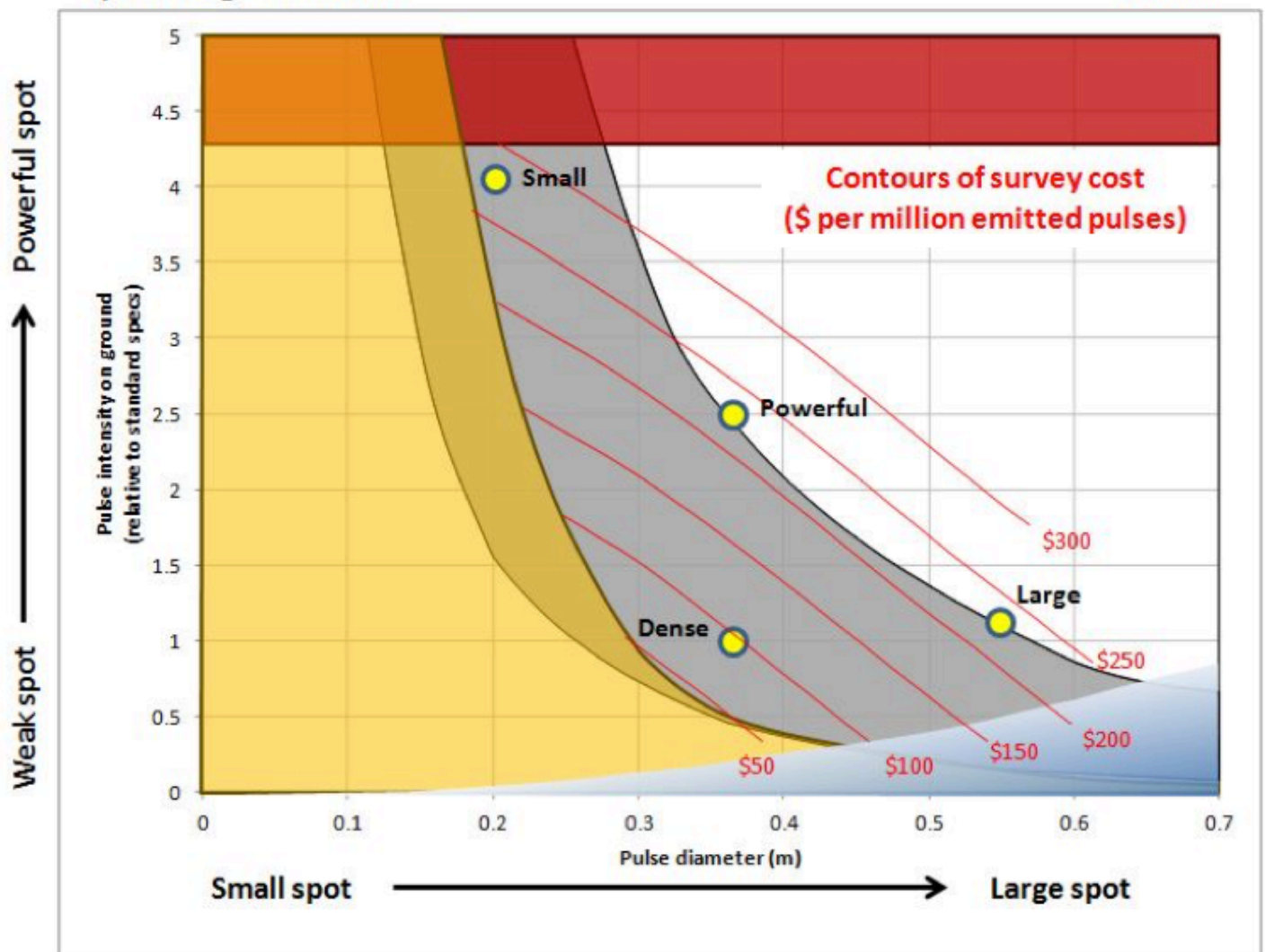


FIGURE 3. The range of LiDAR pulse specifications available for the Optech Pegasus is shown in grey, bounded by power availability (white), nominal laser safety regulations (red), detector sensitivity (blue) and the speed of the electronics and software associated with analysing returns (yellow). Four experiments were designed to explore the available specification space. Contours of survey cost are illustrated in red and show that the most effective specification for maximising the density of emitted pulses is a low power, moderate diameter pulse (labelled Dense).

this ‘Dense’ specification for the regional survey together with three additional experimental spot specifications for the repeated swath (Table 1).

The Luina LiDAR data presents opportunities for more experiments relating to forest penetration:

- As one swath was repeated (i.e., small spot), the effect of repeating swaths at near nadir could be assessed.
- A swath orthogonal to all the other flight lines for the purpose levelling provided an opportunity to assess the advantage of crossed flight lines.
- One experimental specification was used for the regional survey area, so the effect of overlap at moderate off-nadir angles could be examined.
- The advantage of using a dual LiDAR system could be assessed.
- The effect of differing vegetation types could be studied.

This study is restricted to evaluating the effectiveness of survey specifications associated with only the primary experiments.

REGIONAL SURVEY RESULTS

The contractor reported that the survey was successfully completed with a ground point density of ~0.21–0.26 points/m² or ~2 m point spacing (Appendix 4). Data precision (at 68% certainty) was measured by ground control points as 0.10 m in easting and northing and 0.03 m in elevation. Accuracy was not important for this survey but was estimated as 0.10 m (horizontal) and 0.05 m (vertical).

A statistical summary of the ground points is provided in the DEM interpolation processing log (Appendix 6), including:

- Mean ground point density 0.524 points/m² (1.38 m point spacing)
- Median ground point density 0.528 points/m² (1.37 m point spacing)
- Mode ground point density 1.000 points/m² (1.00 m point spacing)

Ground points were separated by an average of 1.4 m, somewhat better than the contractor’s estimate. The difference is due to variation in the method that point density was calculated. More

TABLE 1 Experimental parameters

	Dense	Powerful	Small	Large
Altitude (m)	1800	1800	1000	2700
Pulse Rate Frequency (kHz)	250	100	200	100
Half FOV (degrees)	12.5	12.5	12.5	25
Spot intensity on ground (rel to 'Dense')	1.00	2.50	4.05	1.11
Spot diameter on ground (m)	0.36	0.36	0.20	0.54
Emitted pulse density (points/m ²)	4.61	1.84	3.16	1.23
Cost to obtain the emitted pulse density of the 'Dense' specification (\$ per million emitted laser pulses)	96	240	295	240

detailed statistics show that 43% of ground points were separated by more than 2 m, 30% by more than 4 m, 17% by over 8 m and 3% by more than 16 m (Table 2).

The ground points were converted to a 1 m DEM using minimum curvature (spline) interpolation. The details are provided in Appendix 5 Spline interpolation and Appendix 6 DEM interpolation logs.

The resulting hillshaded DEM highlights built infrastructure associated with mineral exploration, mining and forestry (e.g., Fig. 4), geological features including bedding traces (e.g., Figs 5–7) and features associated with river processes and landslides. Areas underlain by Oonah Formation have bedding characterised by subtle rounded micro-scarps with less common asymmetric but more prominent scarps, reflecting variation in sandstone:siltstone ratio. Bedding features in areas underlain by Luina Group are less common but more prominent, indicating highly contrasting erosional resistance of volcanic flows, intrusions and carbonates in a uniform background of mudstone.

TABLE 2 Ground point separation results for the Luina survey

Point spacing (m)	Proportion of points (%)
0–0.5	33.536
0.5–1	11.461
1–2	11.783
2–4	12.355
4–8	13.745
8–16	13.896
16–32	0.829
32–64	2.193
64–125	0.193
125–256	0.005
256–512	0.003
>512	0.001

The Luina LiDAR project included a sub-project to develop interactive tools to estimate bedding orientation from digitised curvi-linear features in the DEM (Appendix 7: MOI tools). The results were used in compiling the 1:25,000 geological maps of Luina and Waratah (Everard and Cumming, 2016a, b).

EXPERIMENT RESULTS AND DISCUSSION

Results for the primary experiments were calculated for a representative subset of the repeated swath with a north–south flight line at 364500mE, from 5417500 to 5418000mN (GDA94). The terrain, vegetation and geology was typical of most of the region, and the ground point density in the subset (using the 'Dense' spot specification) was 0.34 points/m² or 1.7 m point spacing, 15% less than that a comparable measure for the regional survey. This is understandable as the regional survey included a nominal 30% swath sidelap/overlap and contained areas that were covered by vegetation that were more transparent to LiDAR than the rainforest that completely covered the subset area.

Off nadir

The effectiveness of off-nadir pulses was tested by measuring the number ground points returned with varying off-nadir angles in a representative area (5417500 to 5418000mN, GDA94) using the 'Small' spot specification, which used a 50° full field of view (FOV), 25° either side of nadir. The predicted spot characteristics are presented in Appendix 1, Figure A1.3.

Experiment results: Ground points returned for off-nadir angles 0–25°

The maximum number of ground returns was located at –6° off nadir, corresponding to the average cross track easterly slope of the terrain. The number of ground returns declined at an average rate of 2% per degree off nadir from this maximum (Fig. 8). This result is broadly in agreement with experiments by Leica Geosystems (2006; and Appendix 1), but does not show an increasing rate of decline in the number of ground returns beyond 10° off nadir.

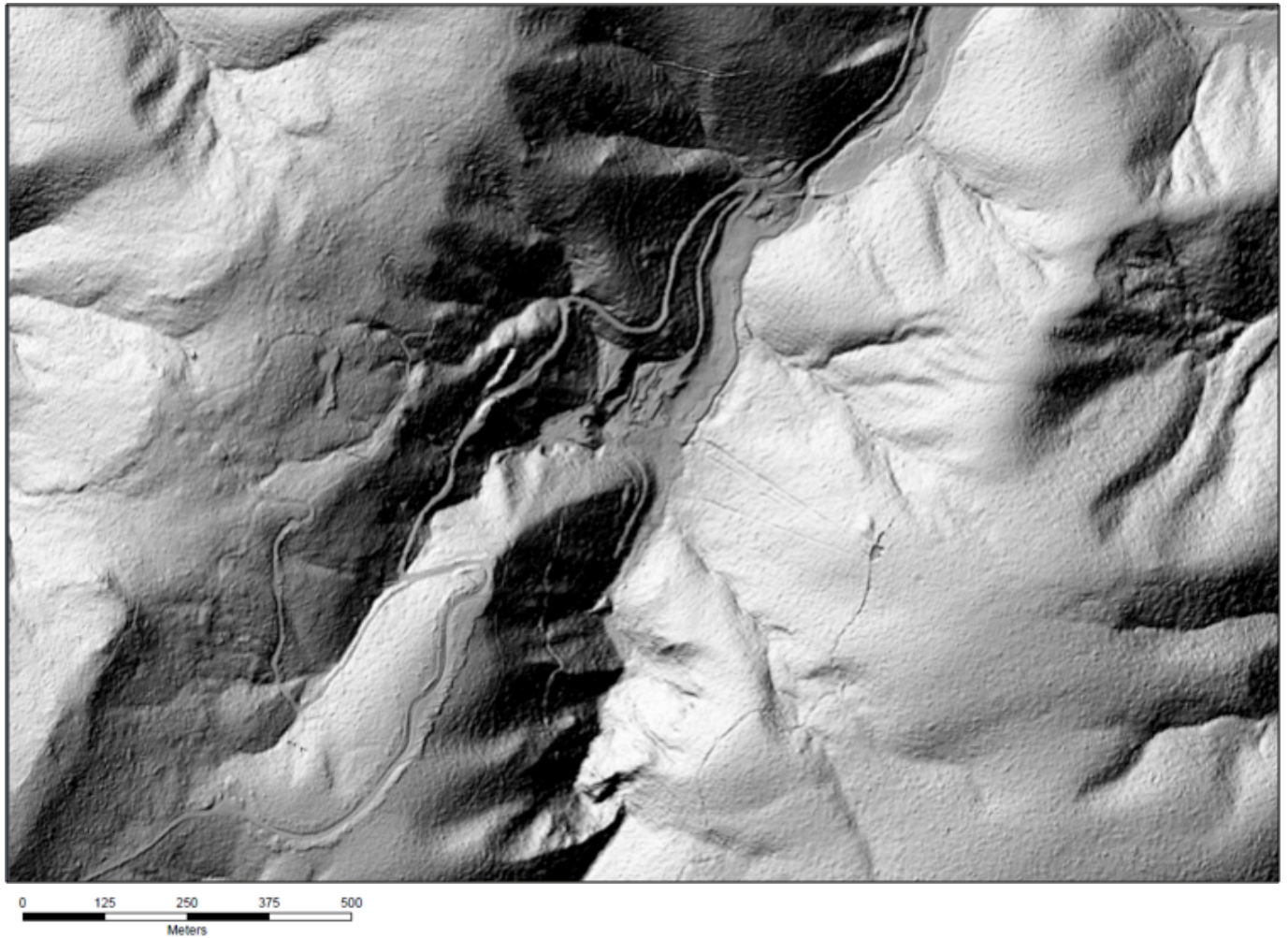


FIGURE 4. This hillshaded DEM of the Magnet mine area in the Luina Group shows ground works associated with historical mining operations. Image is centred on 370460mE, 5410870mN.

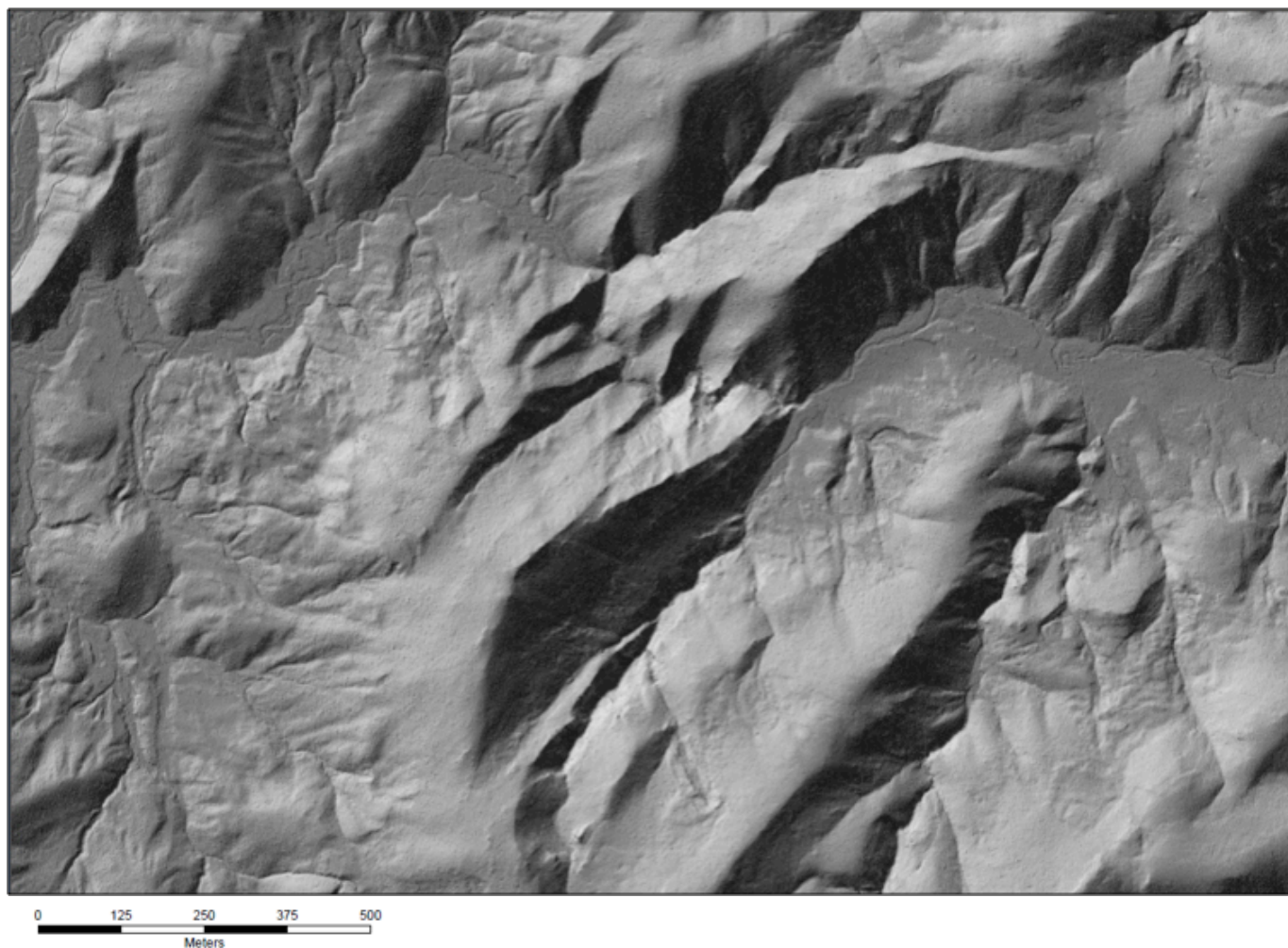


FIGURE 5. The Luina Group in this image is characterised by simple curvi-linear bedding traces prominent in the centre of the image. Some of the traces are not parallel, indicating lithofacies or structural complexity. Image is centred on 364760mE, 5412530mN.

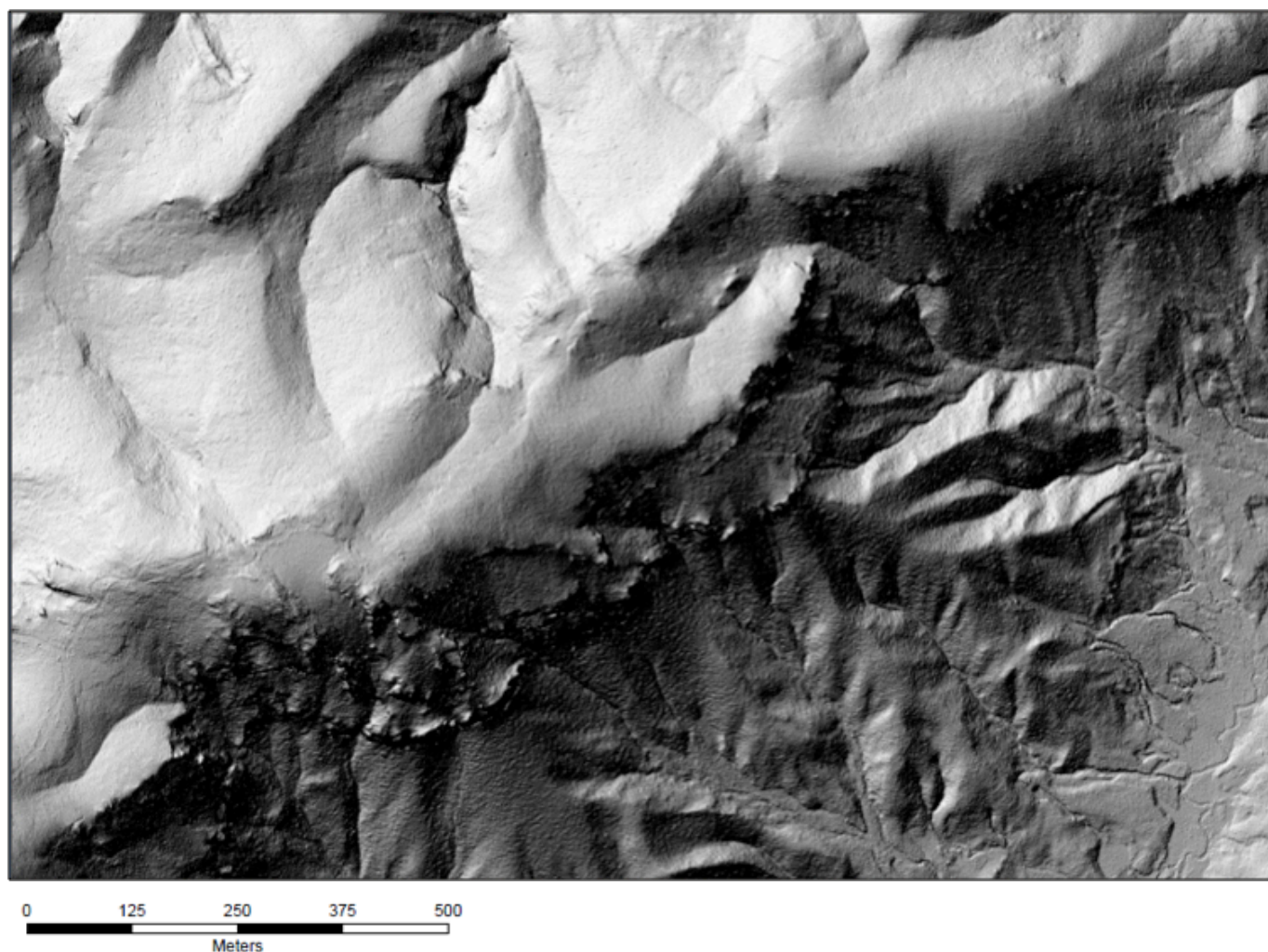


FIGURE 6. The Luina Group in the northern part of Mt Cleveland, which has a summit at bottom left. In the northern part of this scene, large-scale linear features indicate planar bedding, but the prominent curvilinear features in the south may indicate more complex structure. Image is centred on 365900mE, 5410930mN.

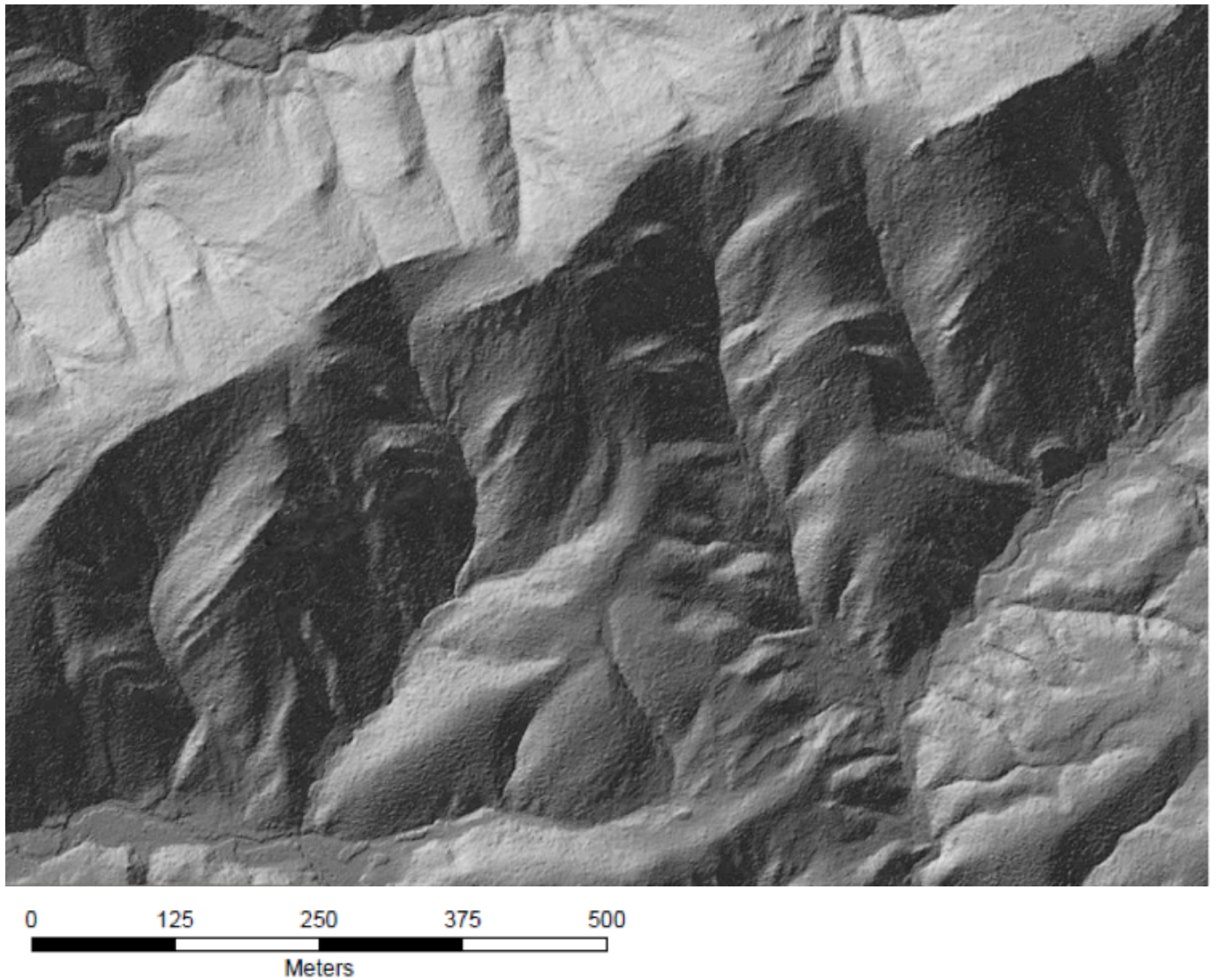


FIGURE 7. Detail in the Oonah Formation illustrating curved bedding traces that indicate folding. The image is a northwest hillshade with a 70% transparent slope image superimposed to accentuate bedding on slopes facing the sun. Image is centred on 366700mE, 5418120mN.

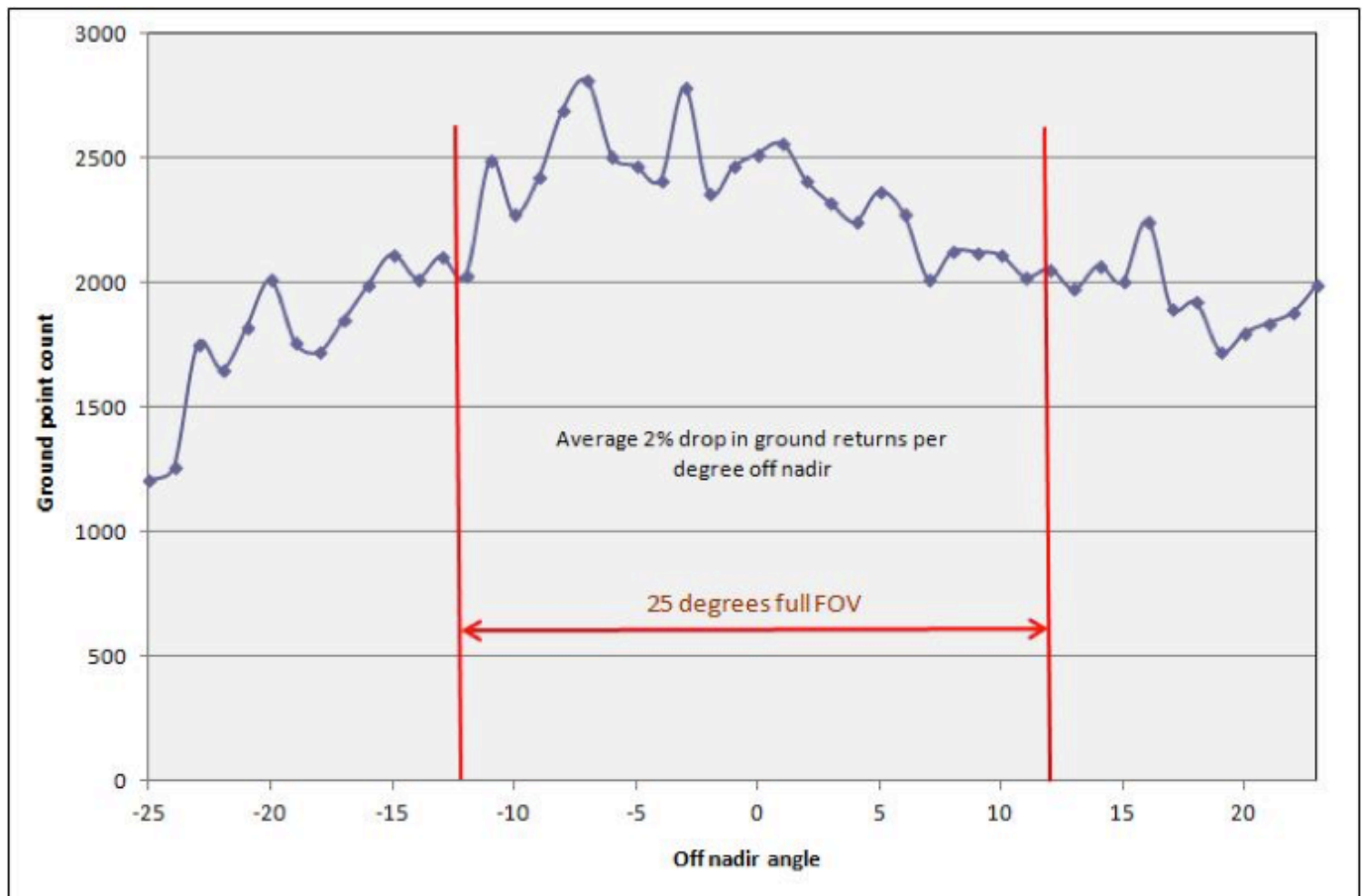


FIGURE 8. Graph illustrating the relationship between off-nadir angle and number of ground returns.

The conclusion from the combined results of this study and those of Leica Geosystems (2006) is that in order to maintain at a ground point return rate of at least 50% that at nadir (beyond which increasing sidelap is a more cost-effective solution), off-nadir angle should be limited to 25°. After allowing for typical ranges in cross track topographic slope (~20°) and aircraft roll (~5°), a practical limit for full FOV would be 25°.

Spot specification

Results were calculated for the representative subset of the repeated swath (364500mE, 5417500 to 5418000mN, GDA94) and off-nadir angle of ≤12° (Table 3).

Ground return/emitted pulse proportions range from 7.3 to 14.3%. For comparison, in northeast Tasmania the equivalent proportion for areas characterised by light forest and little ground cover (e.g., at Mathinna) was 56.4% using 'standard' spot

settings for the era. The most heavily forested terrain covered by the northeast Tasmania LiDAR surveys was at Ringarooma, where 13.6% of emitted pulses were returned from the ground. Similar pulse return results for standard survey specifications over forest at Ringarooma and rainforest with denser canopy and more ground cover at Luina, attests to advances made in LiDAR instrumentation since 2009.

At Luina, the 'Dense' spot specification was least effective at penetrating the forest and returning ground points (Fig. 9). The most effective specification was the 'Powerful' spot, returning nearly twice the proportion of emitted pulses as the 'Dense' specification. A 'Large' spot was found to be more effective than a 'Small' spot: increasing the spot diameter from the 'Dense' specification by 50% (= increasing the spot area by 125%) increased the ground returns by 55% and decreasing the spot size from the 'Powerful' specification by 25% (=

TABLE 3 Experiment results: Ground point density for off-nadir angle $\leq 12^\circ$

	Dense	Powerful	Small	Large
Ground point density at 5417750mN (points/m ²)	0.34	0.26	0.27	0.15
Ground point density/emitted point density	7.3%	14.3%	8.7%	11.8%
Cost per million ground points	\$1260	\$1601	\$3250	\$1933

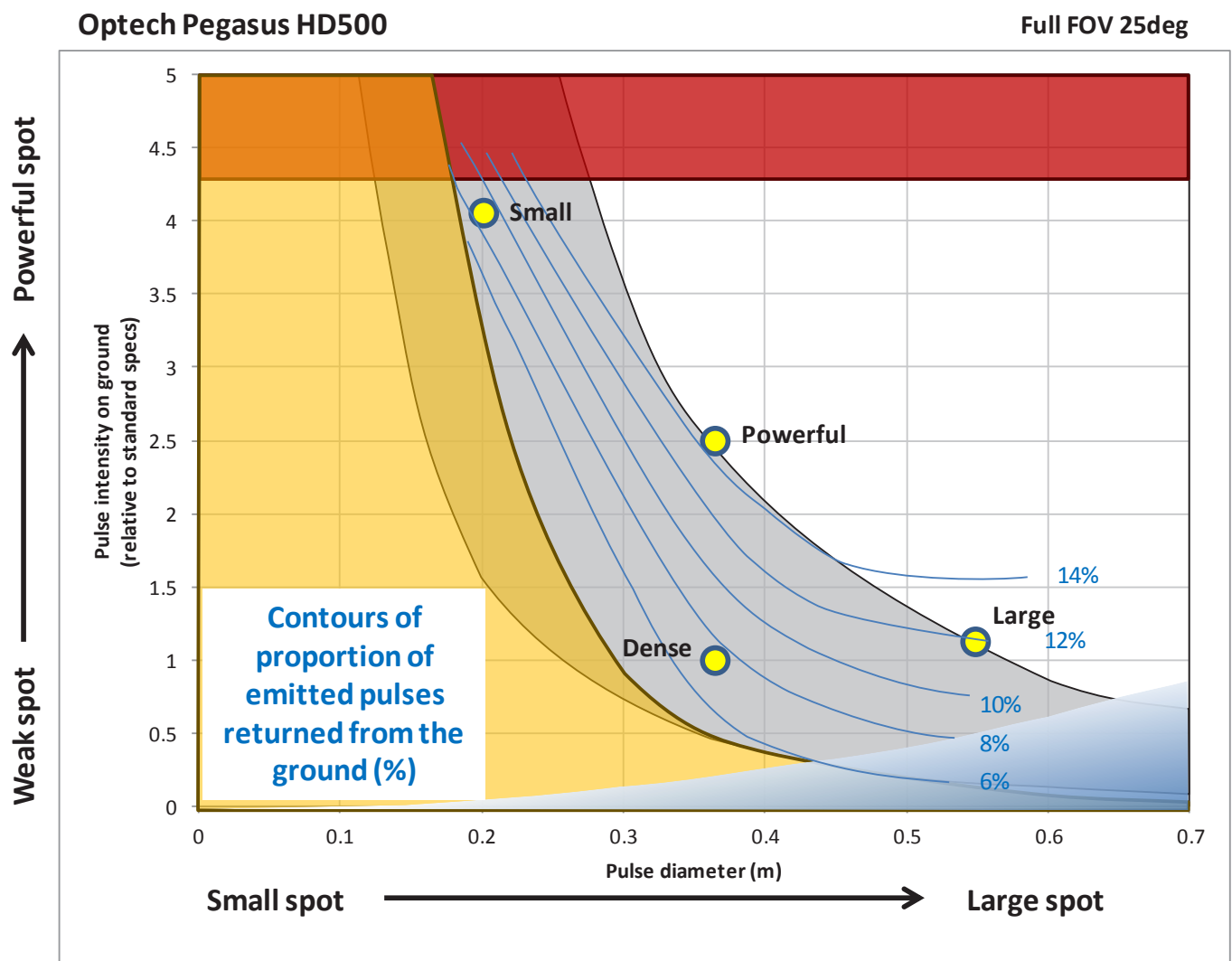


FIGURE 9. The experimental spot specification space contoured by proportion of emitted pulses returned from the ground. The Powerful spot specification was most effective.

decreasing the spot area by 44%) decreased the ground returns by 40%.

The Luina results for ground returns can be compared with those of Leica Geosystems (2006) for North American maple-oak-ash-birch forest. The decrease in the proportion of emitted pulses returned from the ground by reducing the spot size at Luina is at least two times greater than that measured in North America (Fig. 10).

Normalising the results by survey cost gives the cost effectiveness of spot specification (Fig. 11). Although the 'Powerful' specification was nearly twice as effective in returning ground points as the 'Dense' specification, this was more than compensated for by the high emitted point density of the 'Dense' specification, which was the most cost effective specification of all the experiments. Similarly the improved penetration of the 'Large' spot specification is outweighed by its increased cost: increasing the spot diameter by 50% from the standard 'Dense' specification increases the ground returns by 55%, but costs 130% more. The least cost effective specification was the 'Small' spot where a 25% decrease in spot diameter decreases the ground returns by 40% and costs 75% more.

Filling in the gaps

LiDAR ground point coverage in forested areas typically has a patchy distribution, characterised by gaps under large trees (Fig. 12). As a consequence, the quality of a DEM built from such an unevenly distributed, patchy LiDAR ground point distribution will be compromised. For example, in the representative area used to test the effectiveness of spot specification, the average point spacing resulting from the 'Dense' spot specification was 1.7 m, but 32% of the area returned a point spacing of over 3.75 m. At Mathinna, only 2.5% of the surveyed area returned a point spacing similarly greater than the average.

In order to assess the effectiveness of the different spot types to penetrate tall trees, the proportion of ground hits was measured as a function of ground point density (as measured from the combined ground points from all four experiments). Figure 13 illustrates the result, showing that all the experiments have similar performance in areas of high point density, but differences become increasingly apparent as point density decreases.

Figure 14 zooms in on the part of the histogram with low point density (i.e., areas with point density ≤ 0.5 pts/m², or point spacing of ≥ 5 m). The spot setting with the best performance in areas of lowest density of ground returns is clearly the 'Large' spot, which provided 2.2, 2.1 and 1.9 times as many ground returns than the 'Small', 'Dense' and 'Powerful' settings respectively.

When the results of this analysis are plotted as contours in spot specification space similar to Figure 11 it is apparent that the effectiveness of spot specification is strongly sensitive to spot diameter, and contrasts significantly with effectiveness measured by ground returns globally averaged over high and low density return areas. Combining the information from Figures 11 and 14 indicates that increasing the spot diameter by 50% from the 'Dense' setting increases global ground returns by 60% and increases ground returns from areas of low ground point density by 110%.

The cost saving per ground point (in areas of low point density) gained by increasing the spot diameter from the 'Dense' setting by 50% while maintaining spot intensity and emitted point density is 25% (Fig. 15). Although there is a cost saving for areas under tall trees, the cost for the entire survey would be 2.5 times that of a standard survey using the 'Dense' spot specification. The overall increase in survey cost should be weighed against the benefit of improving the resulting DEM under tall trees. That benefit would be an improvement in the 7 m point spacing under tall trees using a 'Dense' spot specification (allowing a 5–10 m DEM) to a 3.3 m point spacing (allowing a 3–4 m DEM).

If a DEM of greater resolution than 3–4 m is required, it would most predictably be achieved by maintaining a large spot size and increasing swath overlap by adding parallel or orthogonal flight lines to ensure all points in the survey area are covered by more than one flight line. This would double the number of emitted and returned ground pulses and improve the DEM to 2 m resolution. The enhanced survey would cost double that of a survey with a 'Large' spot specification and five times that of a standard 'Dense' spot specification.

The benefit of an improved DEM under tall trees can be demonstrated by comparing the DEM built

from ground points returned using the 'Dense' setting with another built from ground points returned from all the superimposed experimental swaths. The 'Dense' setting returned a ground point spacing of 7 m beneath tall trees and the addition of ground points from the other experimental swaths improved this to 4.3 m. The resulting hillshaded DEMs, highlighting just the areas under tall trees, are illustrated in Figure 16. It is apparent that the DEM built from more points contains significantly more detail. As the experiment swaths were not micro-levelled, the improved detail may not reveal more geological signal, but the exercise nevertheless illustrates the improvement in resolution and the increased micro-topographic detail that is possible.

It is worth asking how much detail is actually required in a DEM to reveal geology say, similar to that at Mathinna? Cracknell (2009) found that although 1 m data was available, the most useful

image for identifying bedding features in the Mathinna Group was derived from a 5 m smoothed DEM. Thinning Mathinna ground points to a degree and with a spatial pattern similar to that at Luina (i.e., global point spacing of 1.7 m but with a 7 m spacing in the 32% of the area under the tallest trees) produces a degraded DEM that still contains all the geological features of a DEM built from the un-thinned ground points (Fig. 17a, b). If similar geological features exist at Luina, they should be apparent in the regional DEM (using the 'Dense' spot specification) with the same global point spacing of 1.7 m and 32% of the area having a 7 m point spacing (Fig. 17c). The fact that the Luina regional LiDAR (hillshaded) DEM does not contain large areas characterised by Mathinna-type bedding features indicates that they are not present.

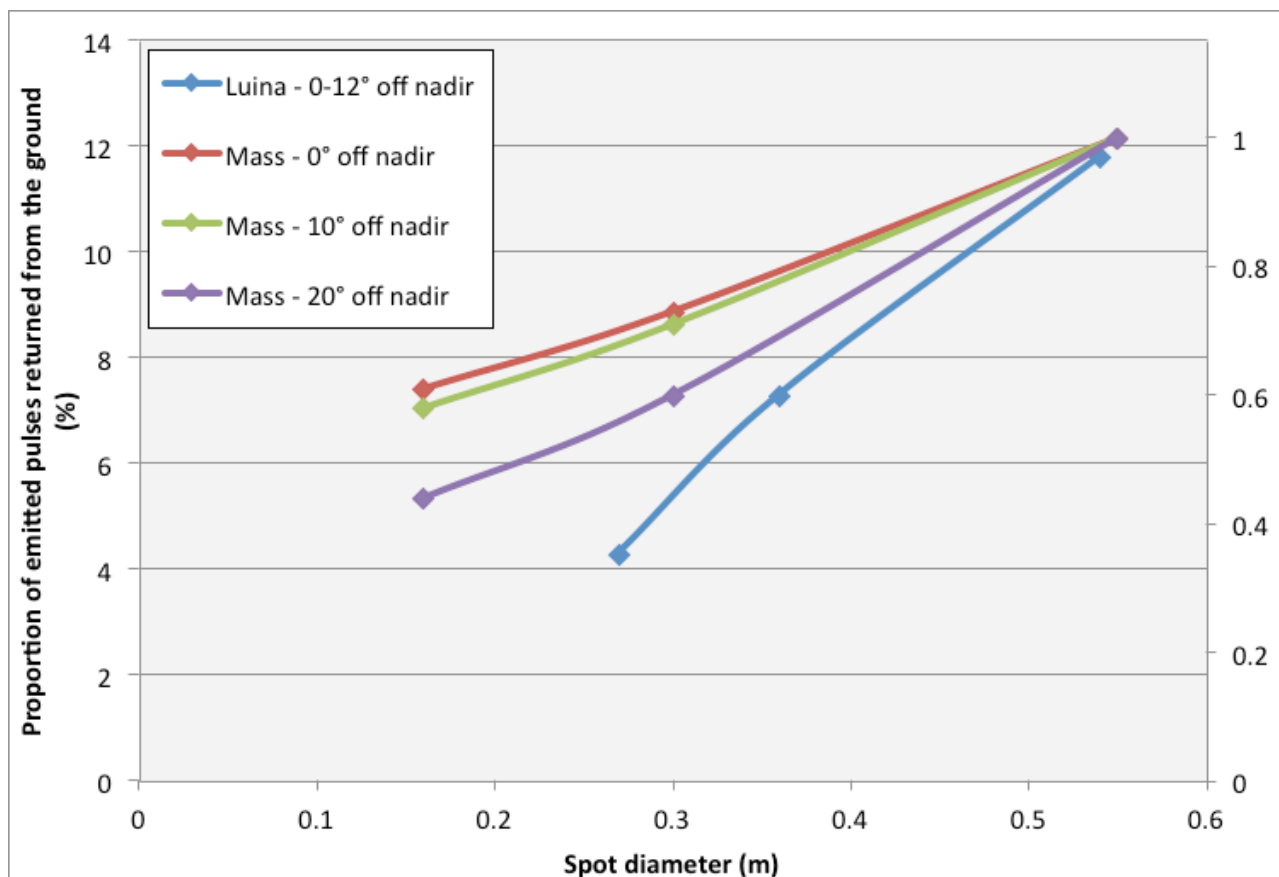


FIGURE 10. The effect of spot size on forest penetration is plotted for Luina and North American forests. In the Massachusetts experiment (Leica Geosystems, 2006), halving the spot size decreased forest penetration near nadir by 25%, but at Luina the decrease was over 50%. The y axis on the left relates to the Luina data and the y axis on the right relates to both the Luina and Massachusetts data. While the Luina results are for all returns $\leq 12^\circ$ off nadir, the Massachusetts results are categorised by off-nadir angle.

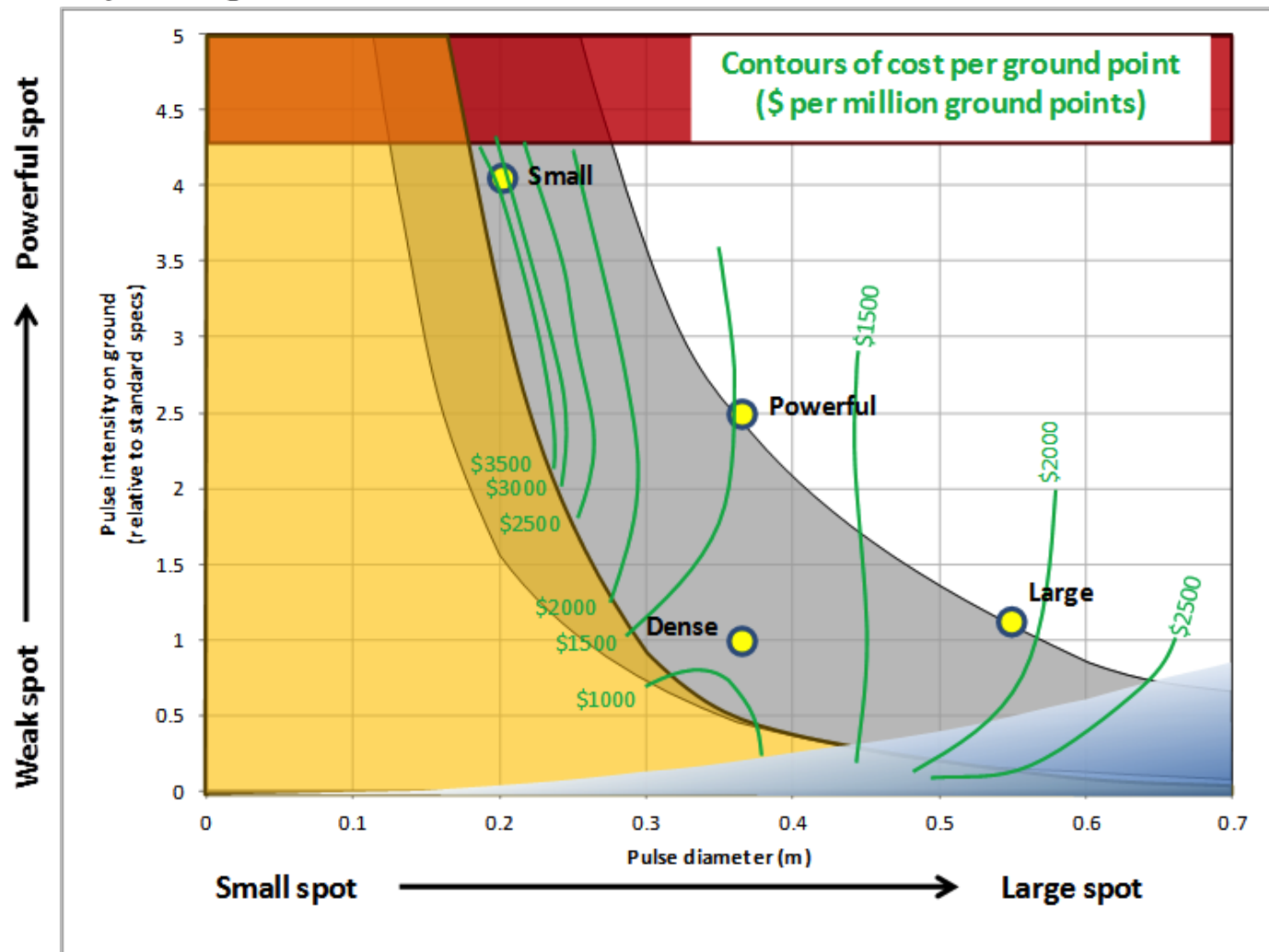


FIGURE 11. The experimental spot specification space contoured by cost per ground point.

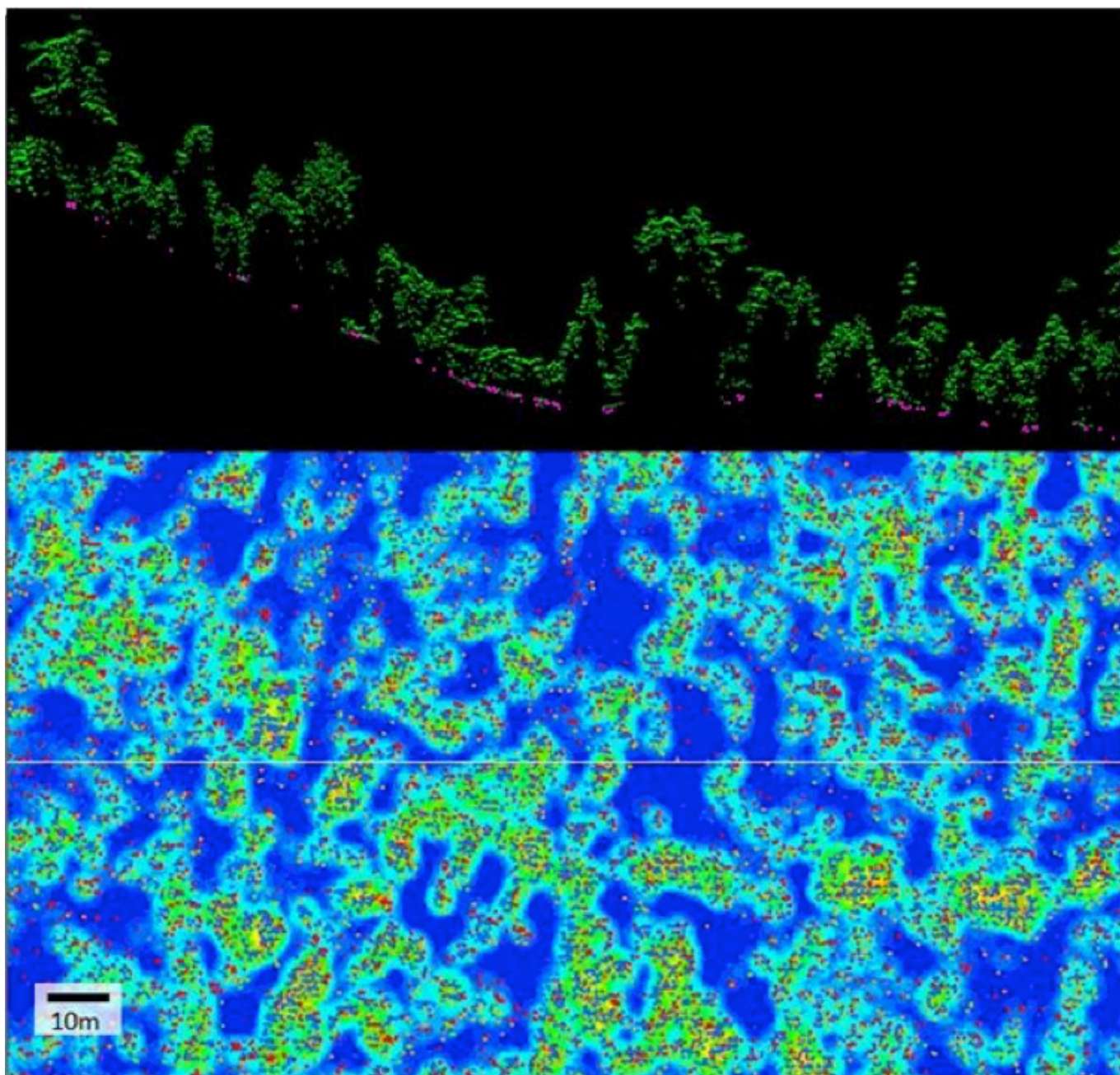


FIGURE 12. Top: Cross section of the LiDAR point cloud in typical forested terrain. Ground points are illustrated in pink and are absent under tall trees. The location of the cross section is indicated with a horizontal white line on the lower map, which illustrates ground point density increasing from blue through green to red. The boundary between blue and green corresponds to a point density of 0.07 pts/m², equivalent to point spacing of 3.75 m). LiDAR ground points from the four experiments are superimposed (Dense = red, Powerful = orange, Small = blue, Large = green). Cross section location: 364814nE, 5417648nN to 364994mE, 5417720mN. The map shows that LiDAR ground points are sparse beneath tall trees and highly concentrated elsewhere.

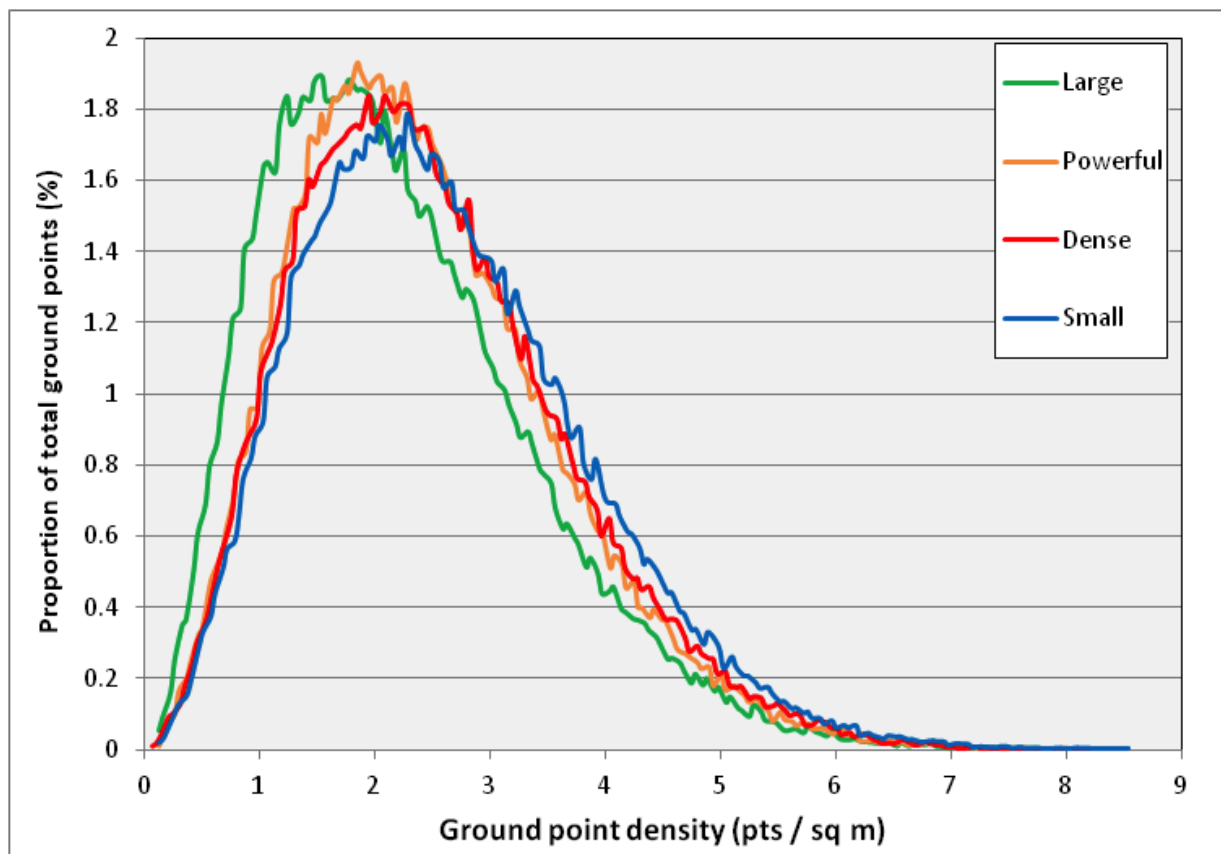


FIGURE 13. Histogram of ground points as a function of ground point density. Ground point density is calculated on the combined ground points from all experiments in the area 364670mE, 5409010mN to 364828mE, 5409490mN with the ESRI Point Density tool using a search radius of 2.5m and cell size of 0.25m. To convert from this point density to the equivalent large-scale measure used elsewhere in this report, divide by 14.2.

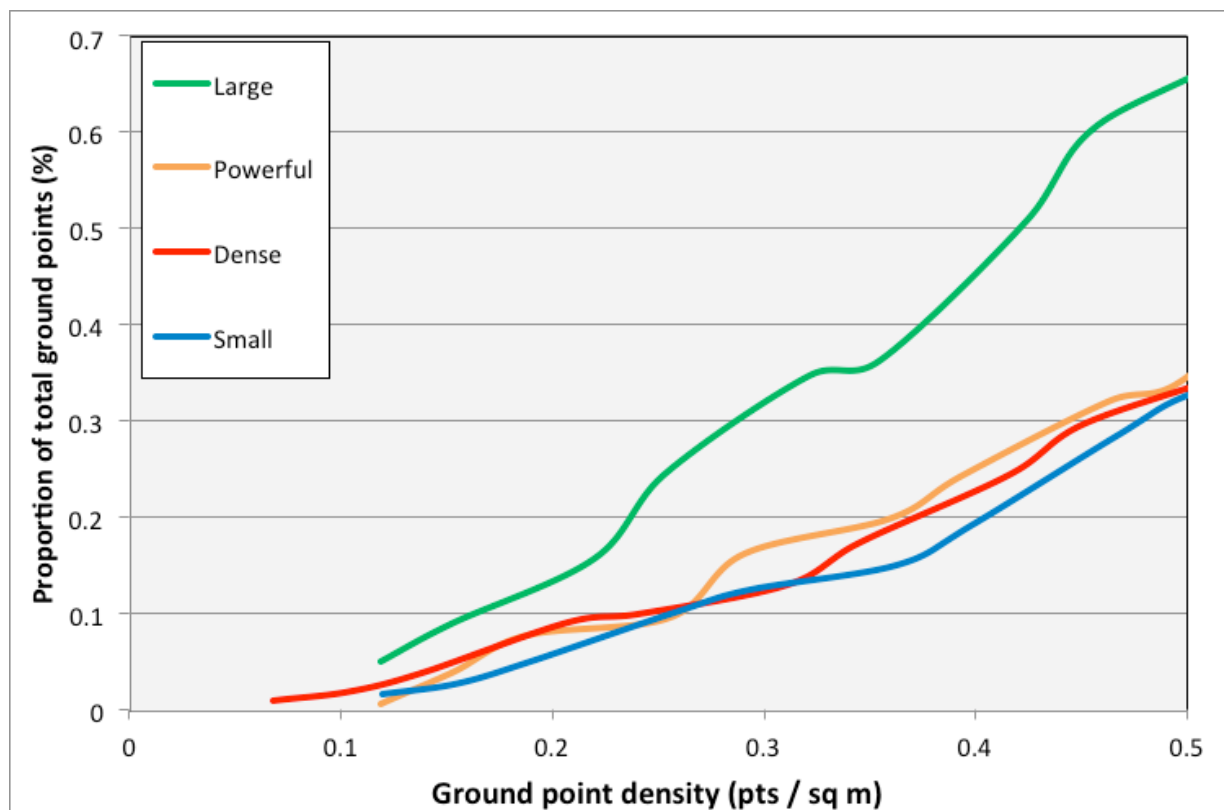


FIGURE 14. Histogram of ground points for areas of low ground point density. A large spot specification performs twice as well as other settings.

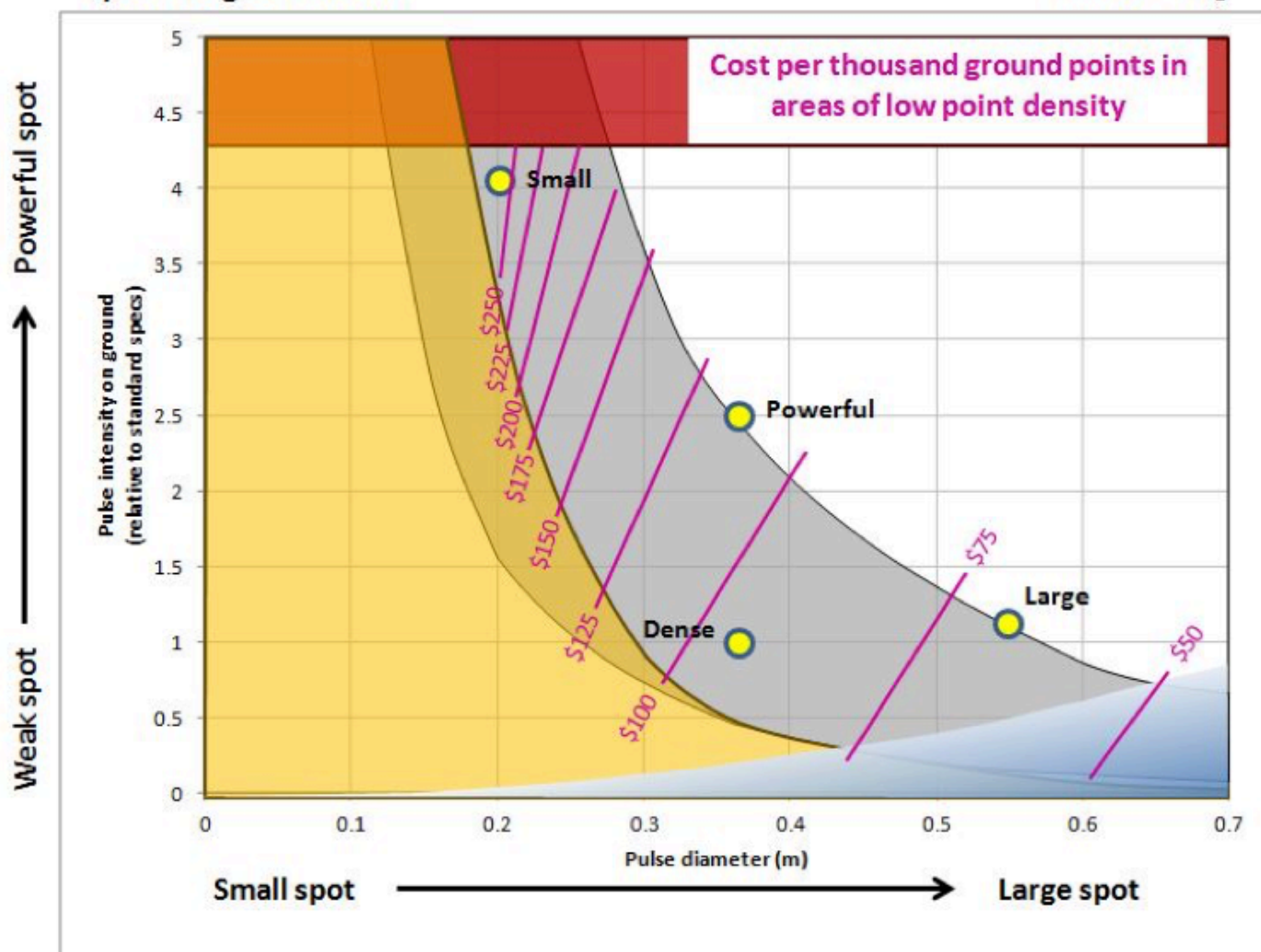


FIGURE 15. The experimental spot specification space contoured by cost per thousand ground points in areas of low ground point density, i.e. under tall trees. The cost is strongly dependent on spot diameter.

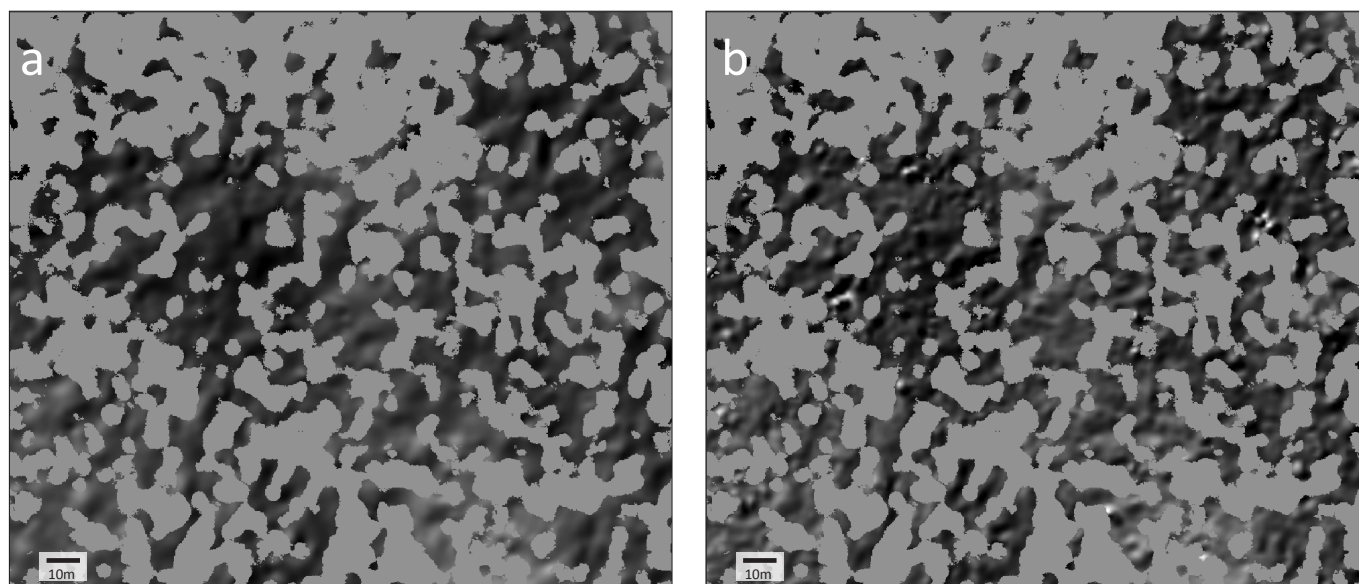
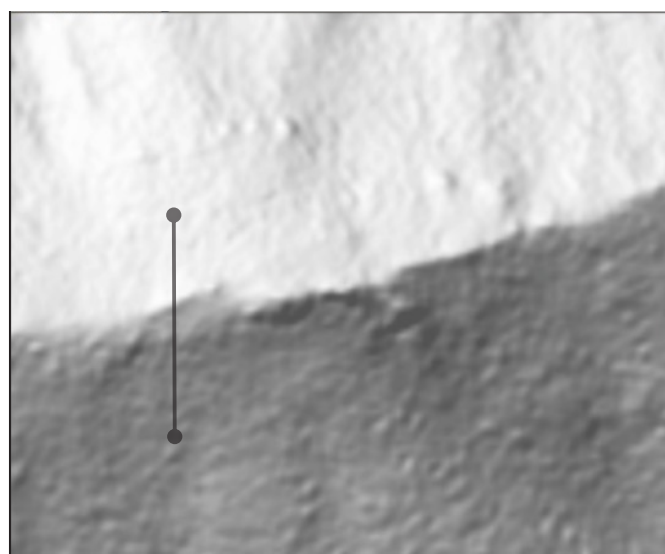
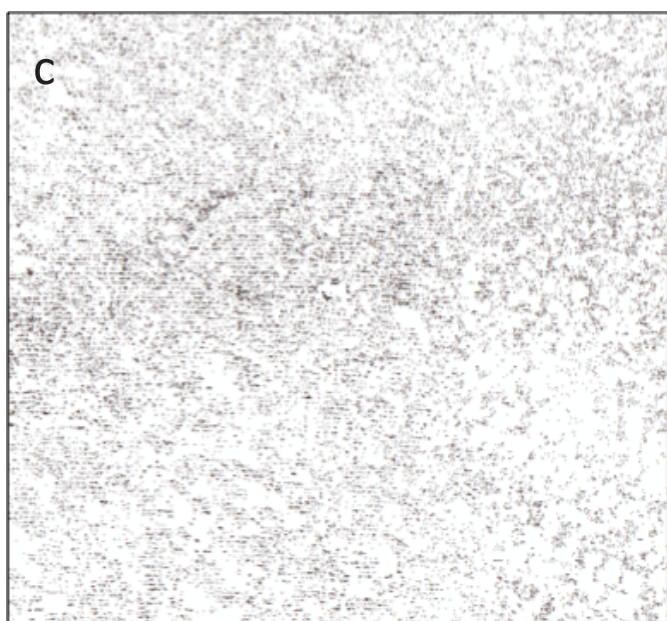
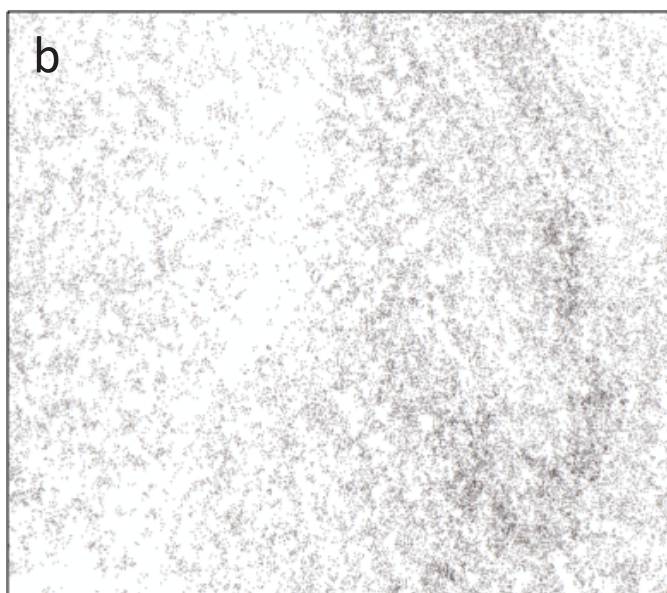
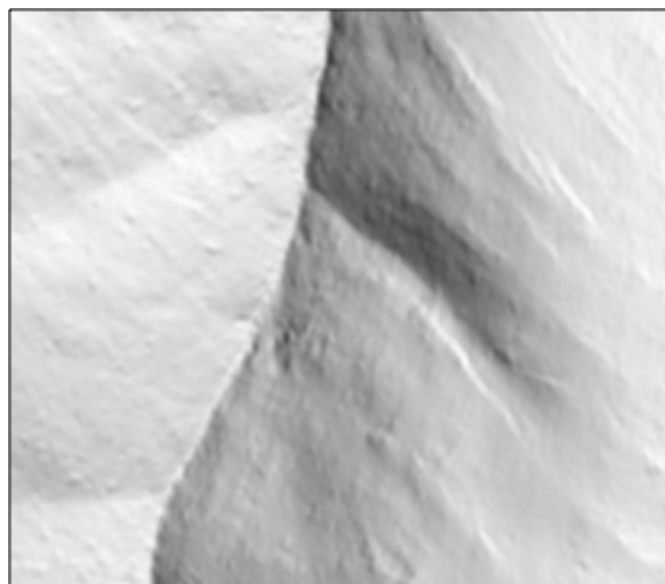
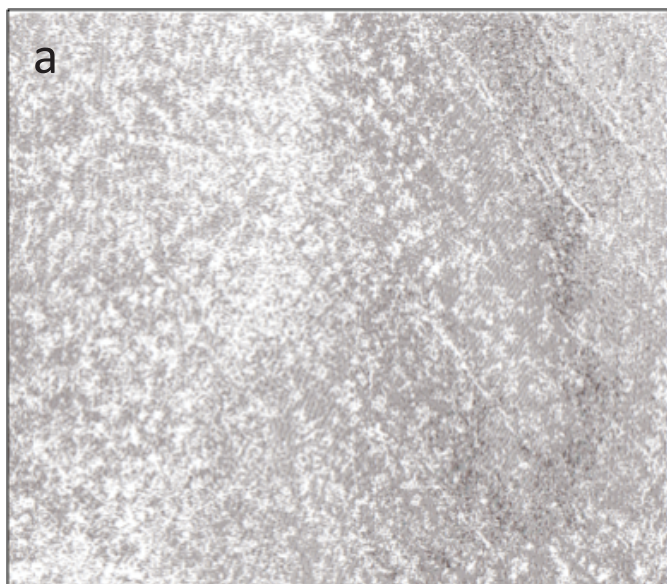


FIGURE 16. Hillshaded DEMs interpolated only from ground points under tall trees (high ground point density areas not under tall trees have been masked with grey); **a.** Dense setting with a ground point spacing of 7 m; **b.** combined experimental swaths with a ground point spacing of 4.3 m. The image extents are 364814mE, 5417648nN to 364994mE, 5417819 mN.

FIGURE 17. Opposite page. Hill-shaded DEMs of portions of the Mathinna and Luina LiDAR surveys built from varying ground point density distributions. **a.** Mathinna DEM built from the original global point spacing of 1 m; **b.** Mathinna DEM built from a global point spacing thinned to 1.6 m and with low density areas which cover 32% of the area having a point spacing of 7 m; **c.** Luina DEM built from similar ground point distribution as **b.** Ground points are illustrated next to each DEM and the locations of cross sections illustrated in Figure 14 are shown in **b** and **c.** The image extents are 364814nE, 5417648nN to 364994mE, 5417819 mN for Luina and 568241mE, 5404471mN to 568647mE, 5404800mN for Mathinna.



Effect of ground cover

A detailed study of the LiDAR point cloud returns at Mathinna and Luina reveals systematic differences. Luina is characterised by taller trees with a far greater density of returns, the presence of a 60-cm-high vegetation layer close to the ground, a markedly lower density of ground points and gaps in the coverage of ground points under tall trees (Fig. 18). Although the ground vegetation has potential to severely impede laser transmission, it appears that pulses consistently penetrated to the ground, as illustrated by the detailed image from Luina in Figure 18.

CONCLUSIONS

The Luina LiDAR survey was flown over heavily forested terrain using state of the art instrumentation and was successful in obtaining enough laser penetration to permit the interpolation of a 2 m DEM. Hillshaded images of the DEM reveal geological features in accord with experience gained in Tasmanian conditions indicating that a 2–5 m DEM is necessary for geological interpretation.

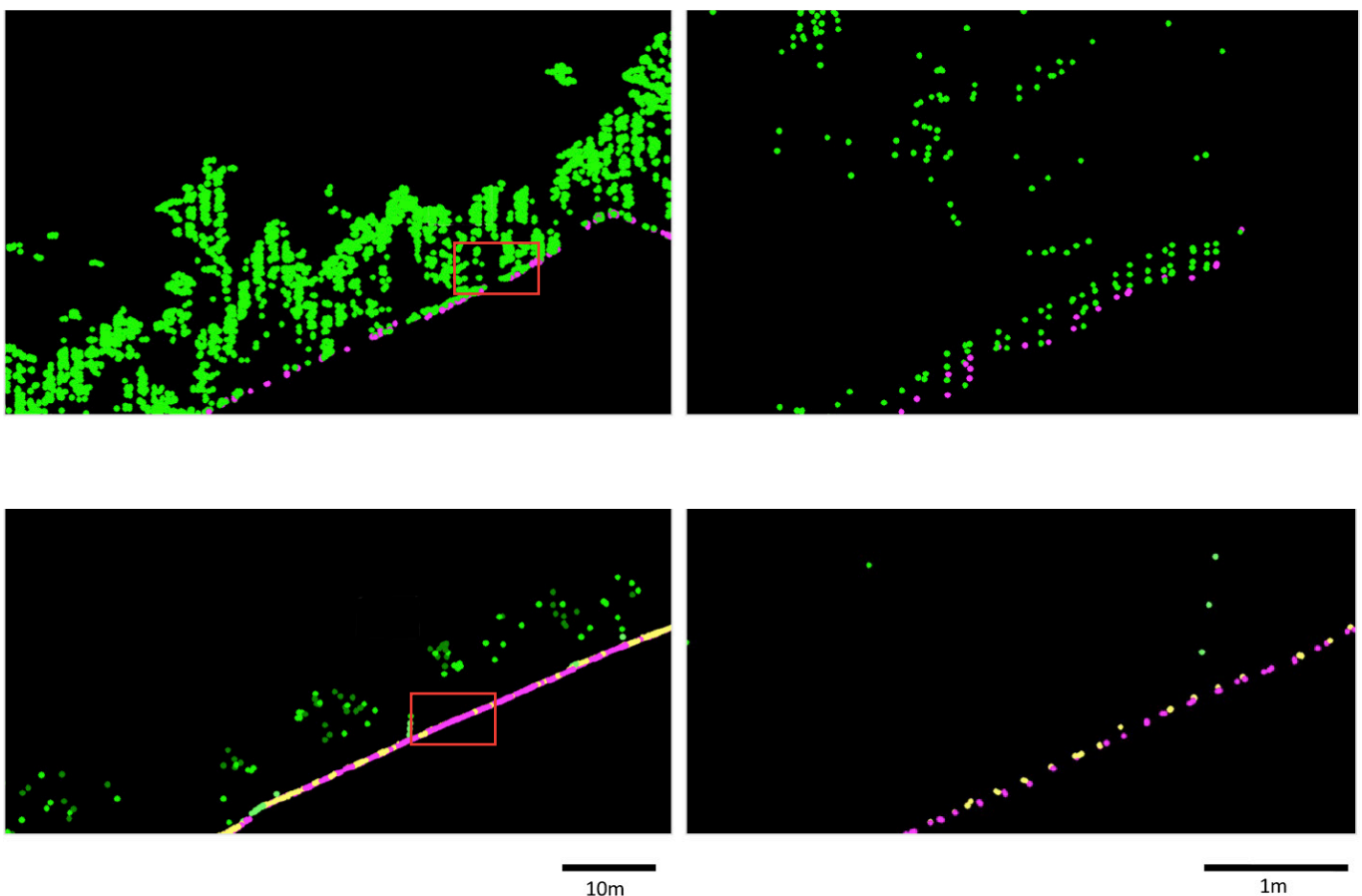


FIGURE 18. LiDAR point cloud cross sections from Luina and Mathinna illustrating differences in ground point distribution. Areas outlined in red are enlarged to the right. Points interpreted to be last returns from the ground are coloured pink. While ground point classification at Mathinna is unambiguous, that at Luina has the potential to be confused by a 60 cm ground cover. Nevertheless it appears that pulses at Luina consistently penetrated through the low cover and ground points are in the main well classified. The sections show all returns in a 2 m east–west thickness and have locations as indicated in Figure 17.

A practical tool to aid the quantitative interpretation of bedding features was developed by Matthew Cracknell. The tool estimates bedding orientation from curvi-linear features identified in the ArcMap environment.

The most cost-effective specification for maximising the total number of ground points is the industry standard setting with a moderate spot size, low power (high pulse rate frequency) and 25° full field of view.

Although industry standard survey settings achieved an excellent average ground point spacing of 1.7 m in the experiment test area, 32% of the area is covered by tall trees where reduced laser penetration resulted in a ground point spacing of only 7 m, compromising its usefulness for geological interpretation.

The most effective spot specification for penetrating tall trees is a large diameter spot, with a 50% increase from the standard setting resulting in point spacing under tall trees improving to 3.3 m. A survey with this spot setting would cost 2.5 times that of a standard survey.

forested sections of the Alpine and Hope faults, South Island, New Zealand: Implications for structural interpretations. *Journal of Structural Geology* **64**: 53–66; doi:10.1016/j.jsg.2013.11.007.

LEICA GEOSYSTEMS 2006. ALS50 mission planning: Special cases – forest floors and power lines. Leica Geosystems Aerial Sensor Workshop presentation. Obtained from Fugro Spatial Solutions Pty Ltd.

NYBORG, M.; BERGLUND, J.; TRIUMF, C.-A. 2007. Detection of lineaments using airborne laser scanning technology: Laxemar-Simpevarp, Sweden. *Hydrogeology Journal* **15**(1): 29–32.

SAS 2014. *SAS/STAT(R) Users Guide*. Viewed at http://support.sas.com/documentation/cdl/en/statug/63347/HTML/default/statug_transreg_sect060.htm

STACKOVERFLOW 2013. *How do I select the smoothing parameter for smooth.spline?*. Viewed at <http://stackoverflow.com/questions/14929268/how-do-i-select-the-smoothing-parameter-for-smooth-spline>

WEHR, A.; LOHR, U. 1999. Airborne laser scanning-an introduction and overview. *ISPRS Journal of Photogrammetry and Remote Sensing* **54**(2-3): 68–82.

REFERENCES

- CHASE, A. F. D.; CHASE, D. Z.; WEISHAMPEL, J. F.; DRAKEC, J. B.; SHRESTHA, R. L.; SLATTON, K. C.; AWE, J. J.; CARTER, W. E. 2011. Airborne LiDAR, archaeology, and the ancient Maya landscape at Caracol, Belize. *Journal of Archaeological Science* **38**: 387–398.
- CRACKNELL, M. J. 2009. Remote sensing geological structures using high resolution Digital Elevation Models. B.Sc. Honours thesis, University of Tasmania, Hobart, Tasmania.
- CRACKNELL, M. J.; ROACH, M.; GREEN, D.; LUCIEER, A. 2013. Estimating bedding orientation from high-resolution Digital Elevation Models. *IEEE Transactions on Geoscience and remote Sensing* **51**: 2949–2959.
- EVERARD J.L.; CUMMING G.V. (2016a). Waratah. Digital Geological Atlas 1:25,000 Series, Mineral Resources Tasmania.
- EVERARD J.L.; CUMMING G.V. (2016b). Luina. Digital Geological Atlas 1:25,000 Series, Mineral Resources Tasmania.
- GREEN D. C.; BOMBARDIERI D. J. 2013. Project summary: LiDAR acquisition and interpretation in northeast Tasmania. Mineral Resources Tasmania Unpublished Report 2013/06: 9 pp.
- LANGRIDGE, R. M.; RIES, W. F.; FARRIER, T.; BARTH, N. C.; KHAJAVI, N.; DE PASCALE, G.P. 2014. Developing sub-5 m LiDAR DEMs for

Appendix 1. The effect of spot size and off-nadir angle

Results from experiments on canopy penetration by Leica Geosystems (2006).

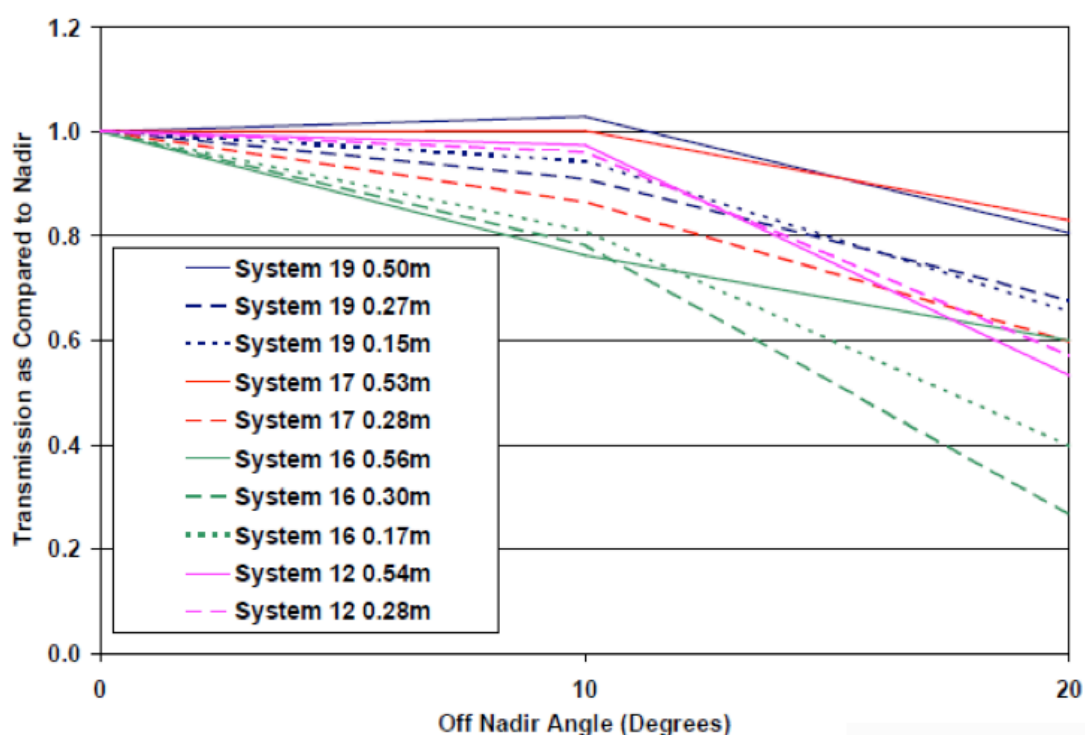


FIGURE A1.1 Results of Leica's experiment to measure the decrease in forest penetration as off-nadir angle increases. The off-nadir effect is more pronounced for smaller spot size for all survey specifications (indicated in the legend by system number and spot size). The experiment was flown in ~2006 using a Leica ALS50 instrument at Leominster, Massachusetts, USA over State Forest comprised of 75-year-old maple, oak, ash, birch and pine. The data was grouped into 0–5, 5–15 and 15–25° samples off nadir.

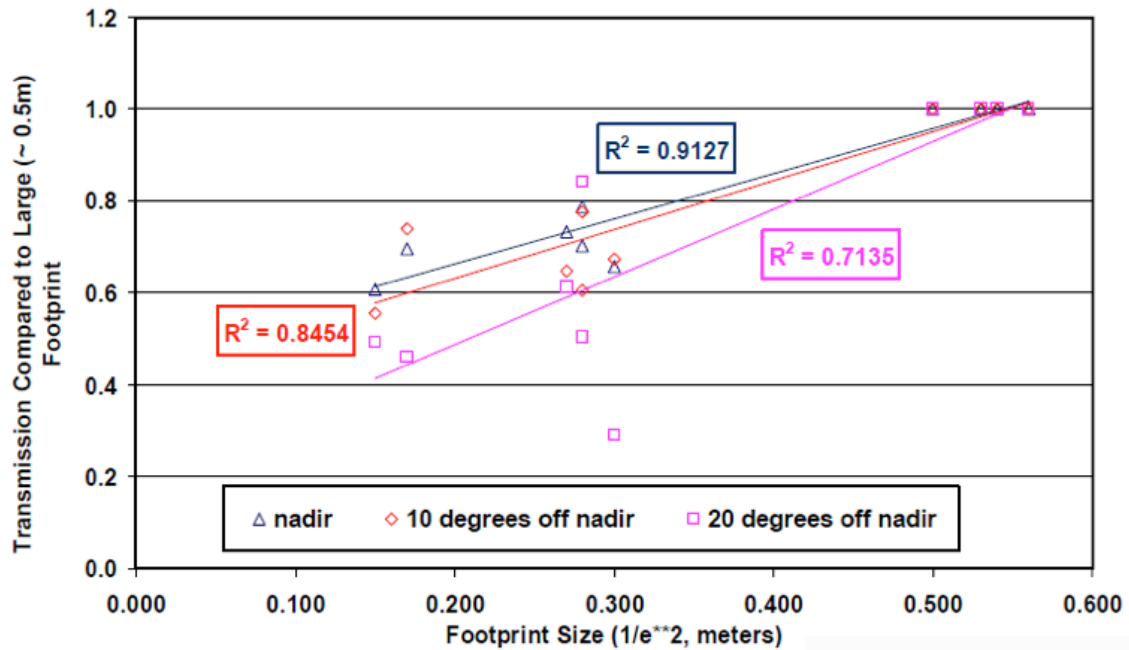


FIGURE A1.2. Results of Leica’s experiment to measure the effect of spot size on forest penetration. Consistent results indicated by linear relationships indicate that halving the footprint size decreases forest penetration by 25% at nadir, increasing markedly to 40% at 20° off nadir. The experiment was conducted in Massachusetts as detailed in Figure A1.1.

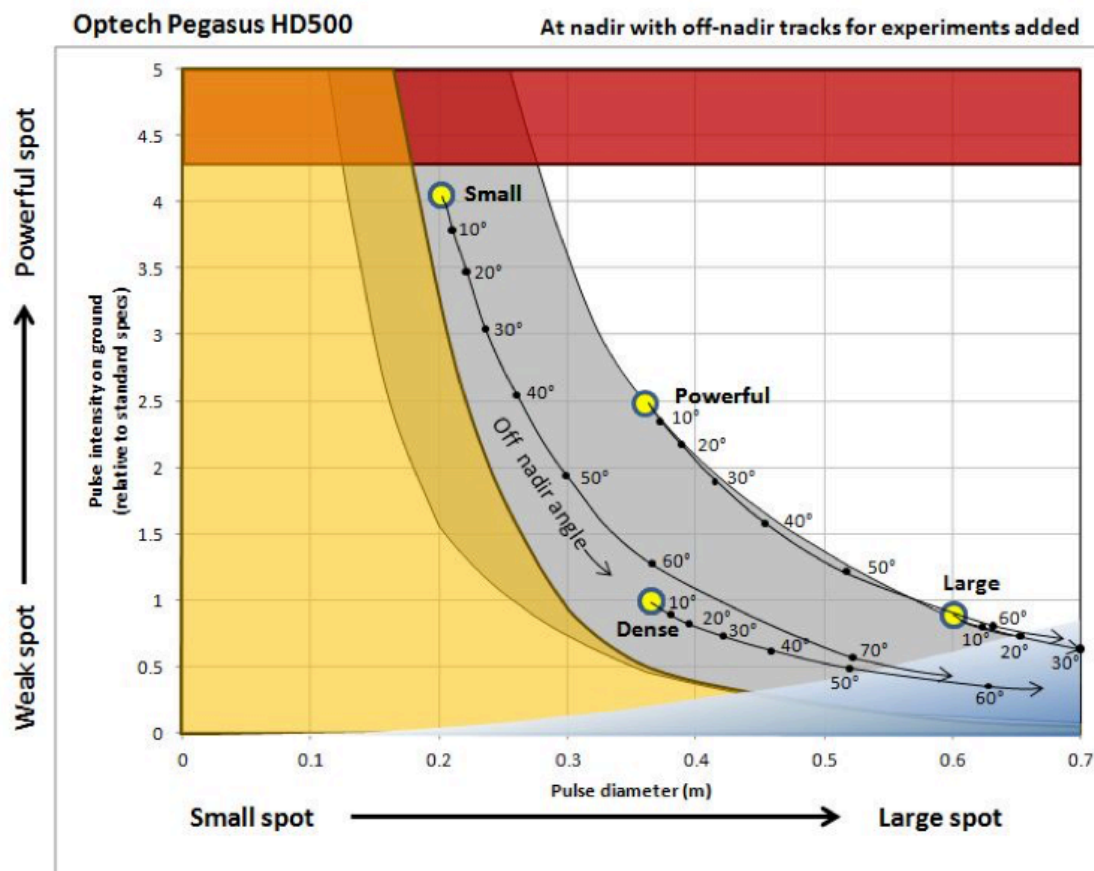


FIGURE A1.3. The calculated effect of off-nadir angle on the laser spot characteristics. The graphs are entirely geometric and based on flat terrain.

Appendix 2. AAM proposal

AAM Ref: 2029402
Commercial In Confidence
©AAM Pty Limited

19 December 2012

David Mannes
Resource Information Manager
Forestry Tasmania
79 Melville Street
HOBART TAS 7000



Suite 1, 1 Oxley Road
Hawthorn VIC 3122
AUSTRALIA
P: +61 (0)3 9572 8750
F: +61 (0)3 9572 8751
info@aamgroup.com
www.aamgroup.com
ABN: 63 106 160 678

Dear David,

Re: MRT Luina LiDAR

We herewith confirm our revised proposal for MRT Luina LiDAR.

Our revised proposal focuses on a solution over a single area using the Optech Pegasus scanner only.

AAM has the technology, know-how, experience and availability of necessary resources to efficiently complete this project using leading-edge technologies. AAM is well-experienced in the successful completion of similar projects.

Our proposal is based on acquiring data in conjunction with our mobilisation for the Forestry Tasmania LiDAR Project, but not at the expense of any significant disruption to our progress on the Forestry Tasmania Project.

Please contact me if you have any questions or require any further information.

Yours faithfully
AAM Pty Limited

A handwritten signature in black ink, appearing to read 'Rohan Potter'.

Rohan Potter
Account Manager

Attachments:


- Proposal Summary
- Our Proposal
- Optech Pegasus scanner information

cc David Green, Mineral Resources Tasmania






MRT Luina LiDAR Project Proposal Summary




Situation

- Pilot project to acquire LiDAR data in an area of heavy vegetation in Tasmania in order to demonstrate the capacity of properly planned and executed LiDAR projects to generate terrain data that can be used for geological modelling and interpretation.
- Luina area of interest of 99 km².



AAM Benefits

- Industry-leading LiDAR technology and experience.
- Demonstrated LiDAR capabilities.
- Optech Pegasus scanner ideally suited for this project.
- Cost-saving of already having scanner and project infrastructure deployed in Tasmania.



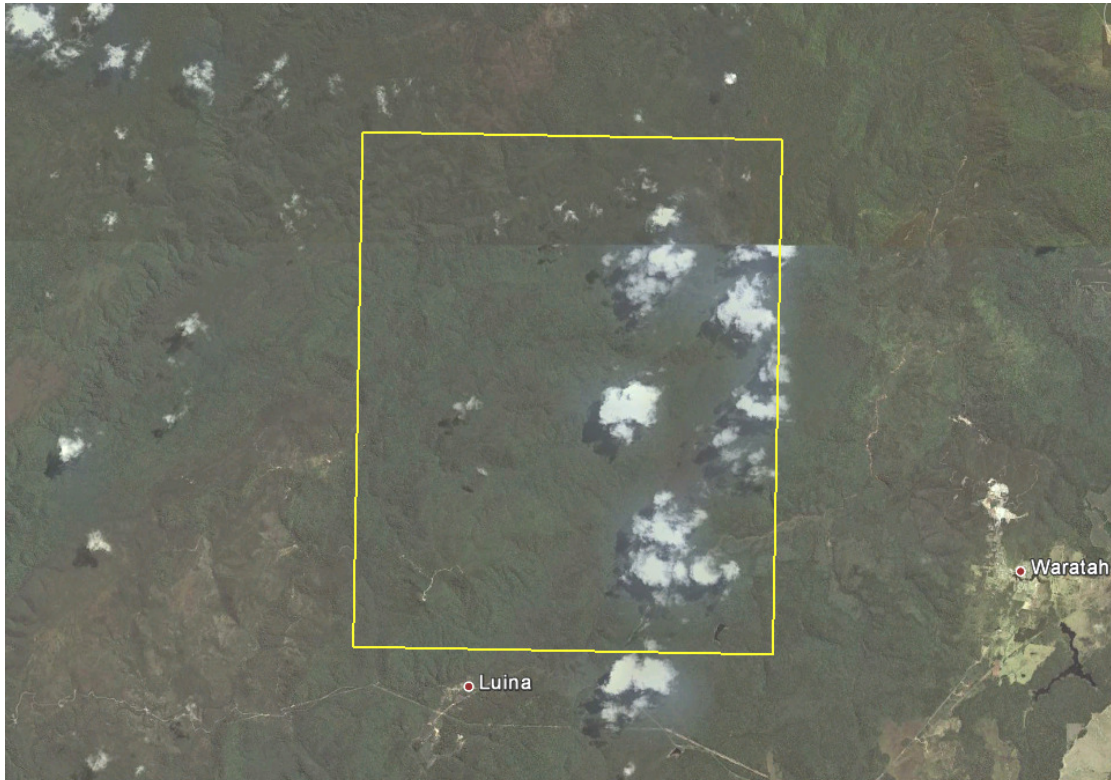
AAM Pricing Summary

- \$42,800 (ex GST) for solution based on acquisition by Optech Pegasus scanner and emitted point density of 4 points/m² for coverage of 99 km², plus two or three swathes with alternative specifications.

PROJECT SCOPE

We understand that the requirement of this project is to acquire LiDAR data in an area of heavy vegetation in Tasmania in order to demonstrate the capacity of properly planned and executed LiDAR projects to generate terrain data that can be used for geological modelling.

We understand that the area of interest is the 99 km² area outlined in yellow in the image below.

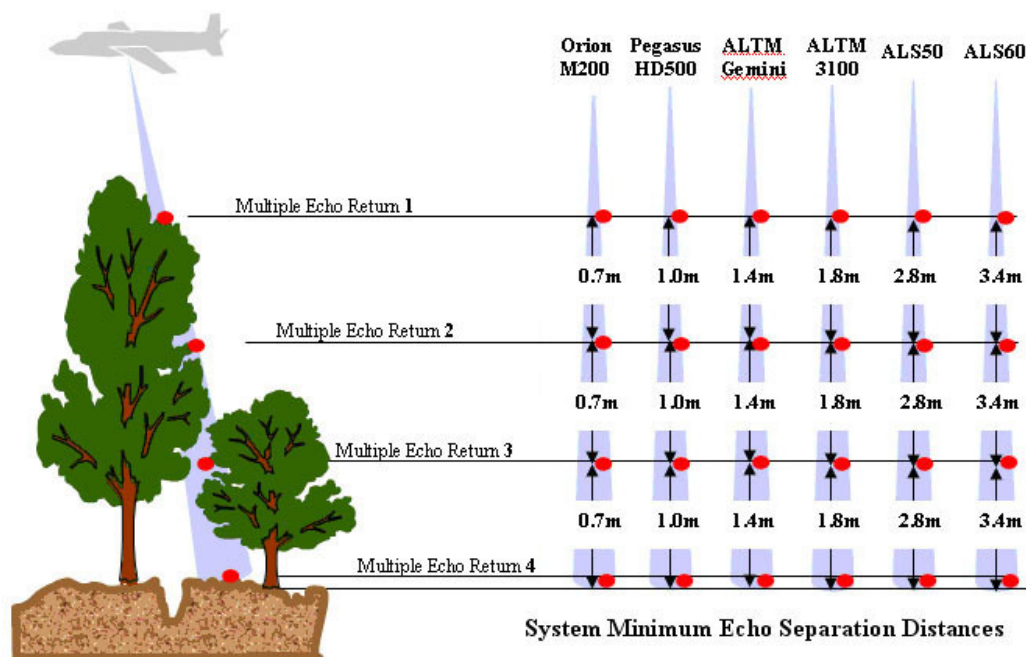


PROPOSED LiDAR SOLUTION

Our proposed LiDAR solution is summarized below:

- LiDAR acquisition to be mobilised in conjunction with Forestry Tasmania LiDAR Project.
- LiDAR data at 15cm vertical accuracy will be acquired using our Optech Pegasus scanner which will be deployed on the Forestry Tasmania LiDAR Project subsequent to an upgrade and commissioning scheduled for early January 2013.
- Complete area of interest will be covered by LiDAR designed for 4 points emitted m². In addition two or three additional swathes will be flown with varied specifications. The varied specifications are to be discussed and confirmed but will likely be any or all of field of view, flying height or pulse rate.
- Data will be georeferenced using a GPS base station solution.
- As absolute accuracy has been stated as being unnecessary for this project no test points will be surveyed for this project, although LiDAR data will be acquired to cover areas suitable for subsequent surveying of test points if required.
- Laser strikes will be classified into all ground, thinned ground and non-ground and delivered in LAS v1.2 format.
- Data classification will be manually checked and edited against available imagery or intensity imagery acquired as part of this project.
- Elevation data will be gathered in ellipsoidal heights and will be adjusted to orthometric heights by applying a correction to every data point using Ausgeoid09.

Our LiDAR experience demonstrates that using a narrow beam LiDAR signal the primary factors that influence the number of LiDAR signals returned from ground are pulse rate and echo separation. The Optech Pegasus scanner is capable of high pulse rates and thus increased point density. The echo separations of a range of Optech and Leica scanners are shown below (we would not recommend a Leica scanner (ALS50 / ALS60) for this project). The Optech Pegasus records up to four true returns for each emitted pulse and the pulses emitted from the vertical and forward looking scanner heads can be tagged according to the scanner head from which the pulse was emitted.



We note that using the Optech Pegasus is the most economical way to achieve higher point densities. Higher point densities can be achieved with scanners with lower pulse rates, but require project designs that necessitate significantly more aviation thus causing such solutions to be uneconomical.

Information about the Optech Pegasus scanner is attached.

TIMING

Acquisition with the Optech Pegasus scanner will be dependent on timing of completion of scanner upgrade and commissioning – this is scheduled for early January 2013.

We anticipate delivery of processed data about four weeks from date of acquisition.

FEE

MRT Luina LiDAR (99 km2)	Fee (ex GST)
Acquisition by Optech Pegasus scanner with emitted point density of 4 points/m2, plus two or three swathes with alternative specifications.	\$42,800

- Our fee excludes GST.
- Fee in this proposal refers to deliverables and specifications set out in this proposal.
- The fee and timelines set out in this proposal are valid for 30 days. AAM reserves the right to amend fees and timelines after this time.
- It is anticipated that the Forestry Tasmania terms of engagement that apply to the Forestry Tasmania LiDAR Project will apply to this project, with the exception of the Forestry Tasmania LiDAR Project fee structure.

- Claims for payment will be presented at the project milestones tabulated below:

Project Milestone	Project Payment
1. Project Commencement	20%
2. Completion of Data Acquisition	40%
3. Delivery of Output Products	40%
Total	100%

Key inputs to the project's cost, commencement and product delivery timelines include:

- Finalisation of the project scope and extent by Forestry Tasmania & MRT.
- Receipt of a purchase order for the correct amount.
- Suitability / quality of required client input data.
- Timely payment of all project invoices.

Any issues, changes or delays relating to these key inputs will be likely to result in delays in project commencement and / or project completion and final project price. Lengthy timelines between quotation and project commissioning can also impact on data capture and product delivery.

AAM will appoint a Project Manager to manage and coordinate the day-to-day production of this project. AAM will provide the Project Manager's name and contact details at project commencement. The Project Manager will be overseen by the Account Manager. The Account Manager for this project is Rohan Potter. Both the Project Manager and Account Manager will be available to Forestry Tasmania & MRT.

All aerial survey work is subject to suitable weather conditions. If weather or other unsuitable conditions intervene, AAM reserves the right to reschedule data acquisition, in consultation with Forestry Tasmania & MRT.

CLIENT RESPONSIBILITIES

Forestry Tasmania & MRT will be responsible for providing:

- Confirmation of the project area.
- The prerequisite key project inputs as indicated in Commercial Conditions.
- A project contact available and able to respond to questions as and when they arise.

QUALITY ASSURANCE

AAM operates within an externally accredited ISO 9001 QA system.

Each project process will be performed in accordance with a written work instruction and documented procedure. Each process will be signed off when complete and in conformance with specified limits.

OCCUPATIONAL HEALTH & SAFETY

AAM is fully committed to ensuring the health and safety of all staff and stakeholders working on this project. Our proposed solution fully complies with all statutory and AAM Occupational Health and Safety policies and procedures. Project specific Safety Management Plans and regular "Toolbox" meetings will maximise the safety of all project personnel.

No on-ground field work is required for this project.

CONCLUSION

Our spatial data supports informed decision-making. We trust our proposal satisfies your requirements.

We will be pleased to answer any questions or provide any further information that you may require.

PEGASUS HD500

Summary Specification Sheet



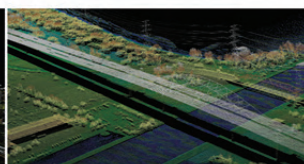
The benchmark in airborne lidar mapping and active imaging technology.

HIGH DENSITY 500 kHz

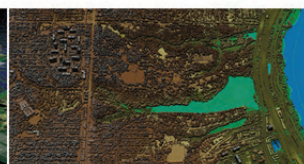
ALTAM Pegasus



Urban Modeling



Asset Management



Topographic Mapping

www.optech.com



Optech

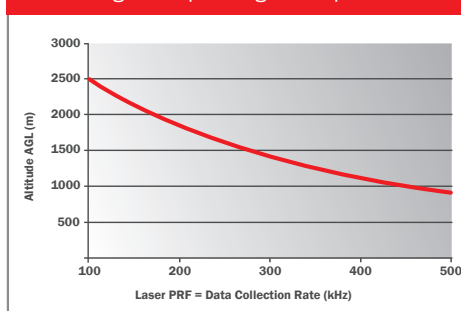
PEGASUS HD500

The ALTM Pegasus Advantage

Pegasus is ideally suited for applications that require maximum collection efficiency in a wide FOV design, while maintaining enhanced target detail and maximum ground density with high range accuracy and precision.

- Dual output laser system for maximum density capability
- High laser sampling rate for enhanced efficiency in XY point distribution
- Extended operating envelope
- “Drop-in” sensor design for unrestricted use of advertised FOV in deep portal installations
- High accuracy and precision independent of pulse rate, enabled by Optech’s iFLEX™ technology
- The latest in tightly-coupled inertial and Virtual Reference System processing technology, enabling steep turns, extended GPS baselines, and the elimination of remote base stations
- Powerful Optech LMS lidar pre-processing software with automated lidar rectification

ALTM Pegasus Operating Envelope



Parameter	Specification
Operational envelope ^{1,2,3,4}	300-2500 m AGL, nominal
Laser wavelength	1064 nm
Horizontal accuracy ²	1/5,500 x altitude; 1 σ
Elevation accuracy ²	<5-15 cm, 1 σ
Effective laser repetition rate	Programmable, 100-500 kHz
Position and orientation system	POS AV™ AP50 (OEM) 220-channel dual frequency GPS/GNSS/Galileo/L-Band
Scan width (FOV)	Programmable, 0-75°
Scan frequency ⁵	Programmable, 0-140 Hz (effective)
Sensor scan product	800 maximum
Beam divergence	0.20 mrad (1/e)
Roll compensation	Programmable, $\pm 32.5^\circ$ (FOV dependent)
Vertical target separation distance	<1.0 m
Range capture	Up to 4 range measurements, including 1st, 2nd, 3rd, and last returns
Intensity capture	Up to 4 intensity returns for each pulse, including last (12 bit)
Image capture	5 MP interline camera (standard); 60 MP full frame (optional)
Full waveform capture	12-bit Optech IWD-2 Intelligent Waveform Digitizer (optional)
Data storage	Removable solid state disk SSD (SATA II)
Power requirements	28 V, 600 W, 21 A
Dimensions and weight	Sensor: 630 x 540 x 450 mm; 65 kg; Control rack: 650 x 590 x 490 mm; 46 kg
Operating temperature	-10°C to +35°C
Relative humidity	0-95% non-condensing

1. Target reflectivity $\geq 10\%$

2. Dependent on selected operational parameters using nominal FOV of up to 50° in standard atmospheric conditions with 24-km visibility

3. Angle of incidence $\leq 25^\circ$

4. Target size \geq laser footprint

5. Dependent on system configuration



US FDA 21 CFR 1040.10 and 1040.11; IEC/EN 60825-1

Optech

300 Interchange Way, Vaughan ON, Canada L4K 5Z8

Tel: +1 905 660 0808 Fax: +1 905 660 0829

www.optech.com

© Optech Incorporated. E&OE. Information subject to change without notice. Printed in Canada. 120924-



Appendix 3: Survey specifications

Option A: Dense spots

Input				
Enter Scan half angle (degrees)	12.5	degrees		
Enter Aircraft speed	60	m/s	120	knots
Enter Altitude (m)	1800	m	5904	ft
Enter system prf (kHz)	250	kHz		
Enter Scan Frequency (Hz)	32	Hz		
Scan angle cut off	0	degrees		
Scan Product	400			
Point Spacing Calculations				
User defined angle for point spacing calculation	12.5	degrees		
Point Distribution - Sawtooth Scan Pattern				
worst case down track point spacing at user angle	0.97	m		
spacing cross track	0.48	m		
Worst case point density at user specified angle	2.12	pt/m ²		
Average point density	4.75	pt/m ²		
MD state (assumes max DIA=4) DIA=4				

Option B: Powerful spot

System Hardware Configuration				
Channel separation downtrack	0.00045	rad		
Channel separation cross track	0.0415	rad		
Input				
Enter Scan half angle (degrees)	12.5	degrees		
Enter Aircraft speed	60	m/s	120	knots
Enter Altitude (m)	1800	m	5904	ft
Enter system prf (kHz)	100	kHz		
Enter Scan Frequency (Hz)	36	Hz		
Scan angle cut off	0	degrees		
Scan Product	450			
Point Spacing Calculations				
User defined angle for point spacing calculation	12.5	degrees		
Point Distribution - Sawtooth Scan Pattern				
worst case down track point spacing at user angle	0.77	m		
spacing cross track	1.39	m		
Worst case point density at user specified angle	0.93	pt/m ²		
Average point density	1.90	pt/m ²		
MD state (assumes max DIA=4) DIA=4				

Appendix 3. cont
Option C: Small spot

Input				
Enter Scan half angle (degrees)	25	degrees		
Enter Aircraft speed	60	m/s	120	knots
Enter Altitude (m)	1000	m	3280	ft
Enter system prf (kHz)	200	kHz		
Enter Scan Frequency (Hz)	32	Hz		
Scan angle cut off	0	degrees		
Scan Product	800			
Point Spacing Calculations				
User defined angle for point spacing calculation	12.5	degrees		
Point Distribution - Sawtooth Scan Pattern				
worst case down track point spacing at user angle	0.89	m		
spacing cross track	0.67	m		
Worst case point density at user specified angle	1.67	pt/m ²		
Average point density	3.39	pt/m ²		
MD state (assumes max DIA=4) DIA=4				

Option D: Large spot

Input				
Enter Scan half angle (degrees)	12.5	degrees		
Enter Aircraft speed	60	m/s	120	knots
Enter Altitude (m)	2700	m	8856	ft
Enter system prf (kHz)	100	kHz		
Enter Scan Frequency (Hz)	24	Hz		
Scan angle cut off	0	degrees		
Scan Product	300			
Point Spacing Calculations				
User defined angle for point spacing calculation	12.5	degrees		
Point Distribution - Sawtooth Scan Pattern				
worst case down track point spacing at user angle	1.16	m		
spacing cross track	1.31	m		
Worst case point density at user specified angle	0.66	pt/m ²		
Average point density	1.27	pt/m ²		
MD state (assumes max DIA=4) DIA=4				

Survey modelling parameters: Option A - Dense spot specification

LIDAR Settings

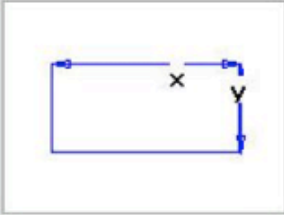
LIDAR Settings | DEM Profile | Statistics

POINT DISTRIBUTION

Nominal Down Track: 0.9646 Nominal Cross Track: 0.4612
 Down Track at Angle: 0.9646 Cross Track at Angle: 0.4612

Mean Pt Density (Pts/m²): 4.61
 Nominal Pt Density: 2.25
 Swath on Flat Ground (m): 654.23

Pt Dist. Angle (deg): 0.0

Scan Pattern: 

SURVEY SETTINGS

Point Density: 0.1 to 50 (Slider: 2.25)

Lidar FOV (deg): 0 to 75 (Slider: 25)

Speed: 120.0 kts
 Sidelap: 30.00 %

Lidar FOV Cutoff (deg): 2.0
☒ Roll Compensation (ON/OFF)

AIRCRAFT SETTINGS

Base Altitude: 1800.0 m
 Range Buffer (m): 100
 Atmospheric Zone (m): 100

☒ AGL ☐ ASL ☐ Terrain Offset

Aircraft Profile Plot

LIDAR SETTINGS

Power (W): MEDIUM

System PRF (kHz): 100 to 500 (Slider: 250)

Scan Frequency (Hz): 0 to 70 (Slider: 32.0)

Target Reflectivity (%): 5 to 100 (Slider: 10.0)

Aided NOHD (m): ☐ 1813.00 Non-Aided NOHD (m): ☒ 307.00

Apply

Appendix 4: AAM survey acquisition report



FORESTRY TASMANIA

LUINA LIDAR TRIALS (FOR MINERAL RESOURCES TASMANIA)

VOLUME 20294A02NOM

Summary

Project

In May 2013 an area of densely forested land in Tasmania chosen for trialing various LiDAR capture specifications in order to ascertain the best fit for Geological Exploration purposes.

Task A (Area A – entire Luina area) was to cover approx 10,000ha at a specification expected to provide suitable terrain definition.

Trials B, C and D were trial swaths (each approx 1,800ha) each with a common flight path centre line, overlapping a part of Area A, but at various specifications, designed to be a LiDAR capture trial.

Data

- Area A - LAS data in tiles, manual classification applied.
- Trial B - LAS data in tiles, manual classification applied.
- Trial C - LAS data in tiles, manual classification applied.
- Trial D - LAS data in tiles, manual classification applied.
- Tile layout in DGN format
- PTC file – Indicates classification types (text file)

CONTENTS

Page Nos.

1.	Data Installation	2
2.	Metadata	3
3.	Conditions Of Supply	5
4.	Validation Plot	6

FORESTRY TASMANIA

1. DATA INSTALLATION

Data format : LAS, DGN, Text
 Number & type of media : USB3 HDD (1TB capacity)
 Number of files on media : 611, viz. 604 LAS files, 4 tile layouts, 1 dir_list.txt, 1 PTC file, & 20294A02NOM_Readme.PDF
 Data formatted on : 27/06/2013
 Disk volume : 20294A02NOM
 AAM Project Manager : Hans Stampa 03 9572 8703
 AAM Account Manager : Rohan Potter 03 9572 8704

README FILE

This document (20294A02NOM_Readme.PDF) is provided as an Acrobat file in this volume.

To open the file, double click on the PDF file to activate Acrobat Reader Software.

Adobe Acrobat Reader may be downloaded from:

<http://www.adobe.com/products/acrobat/readstep2.html>

LOADING NOTES

Data may be copied using a file copy utility such as Windows Explorer or similar.

FILE SIZES AND NAMES

See dir_list.txt for file listing

LAS tiles are named by truncated South West corner coordinate.

SAMPLE LISTING

LAS format is binary and cannot be listed like a text file can. This should be opened in a LAS viewer.

LAS file point classifications levels are formatted to comply with ASPRS Standard LiDAR Point Classes.

0	Unclassified
1	Default
2	Ground
3	Low Vegetation
4	Medium Vegetation
5	High Vegetation
6	Building
7	Low / High points
8	Model Keypoints
9	Water
10	Bridge
11	Error Points
12	Cut Overlap Points
13-31	Reserved for ASPRS Definition

Classes in bold are delivered within this volume

FORESTRY TASMANIA

2. METADATA**DATA CHARACTERISTICS**

Characteristic	Description
Format	LAS
Size	Opt A 2,553,000,000 data points (approximate) Opt B 58,000,000 data points (approximate) Opt C 209,000,000 data points (approximate) Opt D 53,000,000 data points (approximate)
Laser return	1 st , 2 nd 3 rd and last
Laser footprint size	0.2m – 0.7m
Laser mode	Single and Multipulse
Nomenclature	Tiles are named by truncated South West corner coordinate E.g. Opt_A_e3630n54090.las - - Option is area A - - SW Corner at 363000E, 5409000N MGA 55

FLYING PARAMETERS

Area Name	Altitude (m)	Frequency (kHz)	Sub Frequency (Hz)	Full FOV (deg)
A	1800	250	32	25
B	1800	100	36	25
C	1000	200	32	50
D	2700	100	24	25

POINT DENSITY ACHIEVED

Tile	Opt A	Opt B	Opt C	Opt D
e3650n54090				
Ground	0.58m ²	0.26m ²	0.44m ²	0.17m ²
Vegetation	21.16m ²	5.64m ²	18.53m ²	3.71m ²
e3645n54130				
Ground	0.63m ²	0.26m ²	0.46m ²	0.17m ²
Vegetation	22.51m ²	5.23m ²	17.06m ²	3.17m ²
e3650n54175				
Ground	0.57m ²	0.25m ²	0.48m ²	0.14m ²
Vegetation	23.29m ²	5.62m ²	19.32m ²	3.20m ²
e3645n54195				
Ground	0.45m ²	0.21m ²	0.43m ²	0.15m ²
Vegetation	20.22m ²	5.63m ²	22.09m ²	4.09m ²

FORESTRY TASMANIA

REFERENCE SYSTEMS

	Horizontal	Vertical
Datum	GDA94	AHD (TAS1983)
Projection	MGA 55	N/A
Geoid Model	N/A	Ausgeoid98
Reference Point	ST393 on Mt Cleveland 364502.502E 5410020.321N	ST393 on Mt Cleveland 857.53RL
Description	Brass SPM mark No. 2845 in concrete at ground level	

***This data is GDA compliant*****SOURCE DATA**

	Source	Description	Ref No	Date
Survey control	Tritech Surveys	Rapid static GPS	16577D	23.5.2013
Laser Scanning	AAM	4 Trials – See above	20294A15	May 2013
Test points	Tritech Surveys	Leica GPS	16577D	23.5.2013

EXPECTED ACCURACY

Project specifications and technical processes were designed to achieve accuracies as follows:

	Measured Point	Derived Point	Basis of Estimation
Ground control	0.05m		Survey methodology used
Test points (XY)	0.10m		Deductive estimate
Test points (Z)	0.05m		Survey methodology used

Notes On Expected Accuracy

- Values shown represent standard error (68% confidence level or 1 sigma), in metres
- “Derived points” are those interpolated from a terrain model.
- “Measured points” are those observed directly.
- Accuracy estimates of measured points refer to discrete point-mode observations. Observations taken in string-mode can be up to two times less accurate.
- Accuracy estimates for terrain modeling by ALS or photogrammetry refer to the terrain definition on clear ground. Ground definition in vegetated terrain may contain localised areas with systematic errors or outliers which fall outside this accuracy estimate
- Laser strikes have been classified into “ground” and “non-ground”, based upon algorithms tailored for major terrain/vegetation combinations existing in the project area. The definition of the ground may be less accurate in isolated pockets of dissimilar terrain/vegetation combinations.

FORESTRY TASMANIA

LIMITATIONS OF DATA

- Features obscured by foliage or shadow may not appear.
- The definition of the ground under trees or shadow may be less accurate.
- Underground services have not been mapped.

DATA VALIDATION**ALS Data**

- Ground data in this volume has been compared to 21 test points obtained by field survey and assumed to be error-free. The test points were distributed in 1 group to the South of the mapping area and located on clear ground
- Comparison of the test points with elevations interpolated from measured data resulted in:

Mean difference	:	-0.659m
St.Deviation	:	0.03 m
Standard Error (RMS)	:	0.03 m

This mean elevation difference has been removed from the data supplied in this volume
- Data classification has been manually checked and edited against any available imagery.

USE OF DATA

- Intended use : Testing usefulness of LiDAR for geological exploration

3. CONDITIONS OF SUPPLY

The data in this volume has been commissioned by **FORESTRY TASMANIA**.

The data in this volume is provided by AAM Pty Limited (AAM) to **FORESTRY TASMANIA** under the client's Terms of Engagement, which require **FORESTRY TASMANIA** to assume beneficial ownership, subject to the following conditions:

1. This file (Readme_20294A02NOM.PDF) is always stored with the unaltered data contained in this volume.
2. The data is not altered in any way without the approval of AAM. The data may be copied from this file to another.
3. The data is not used for purposes beyond that explicitly agreed in the description of the Services provided by AAM.

Any breach of these conditions will result in the immediate termination of the license issued by AAM, and **FORESTRY TASMANIA** will indemnify AAM from all resulting liabilities.

Any problems associated with the information in the data files contained in this volume should be reported to:

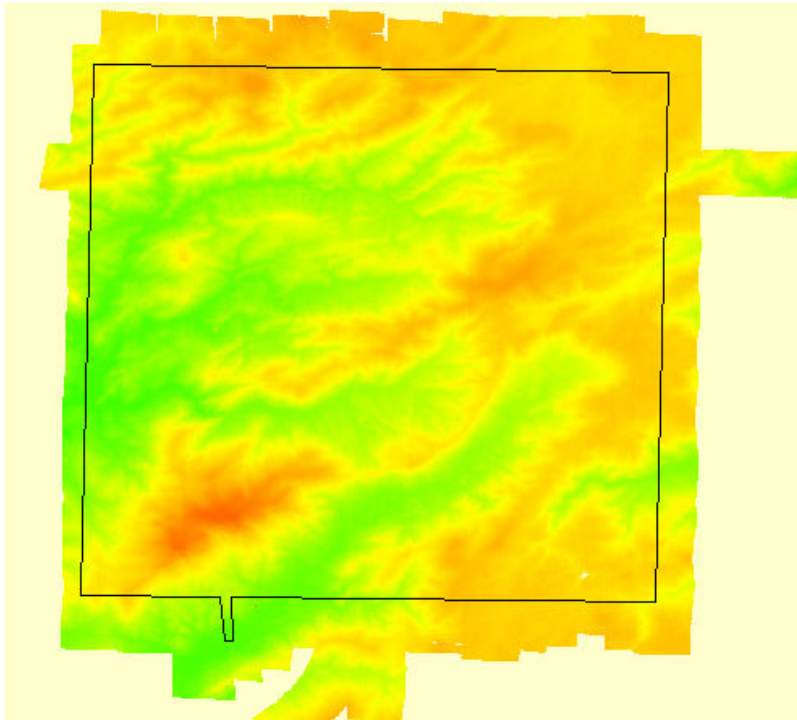
AAM Pty Limited

90 Camberwell Road
 HAWTHORN EAST VIC 3123
 Telephone (03) 9572 8750
 Facsimile (03) 9572 8751
 Email info@aamgroup.com
 Web www.aamgroup.com

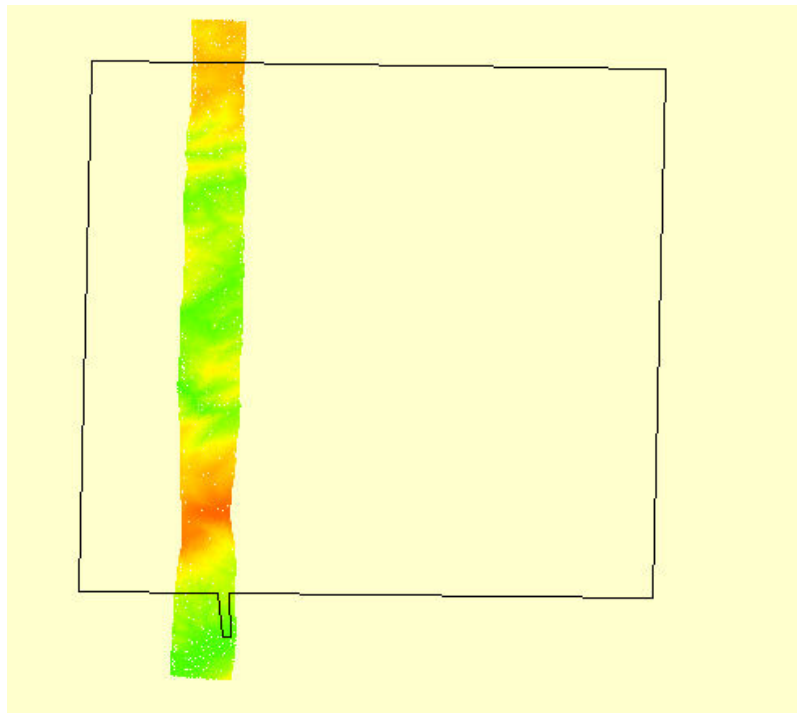
4. VALIDATION PLOT

The purpose is to present an expectation of what is being delivered and that no data is missing.

AREA A

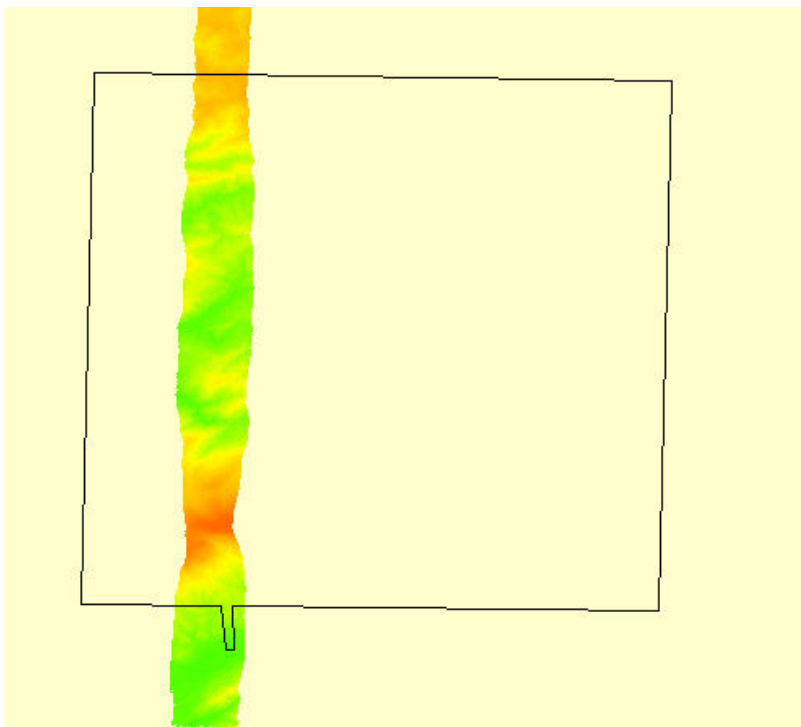


TRIAL B

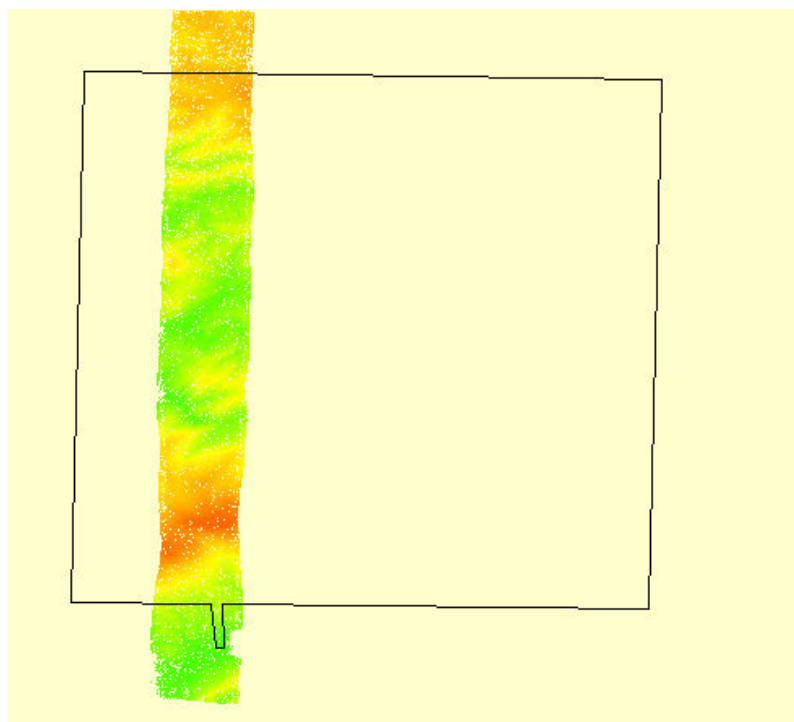


FORESTRY TASMANIA

TRIAL C



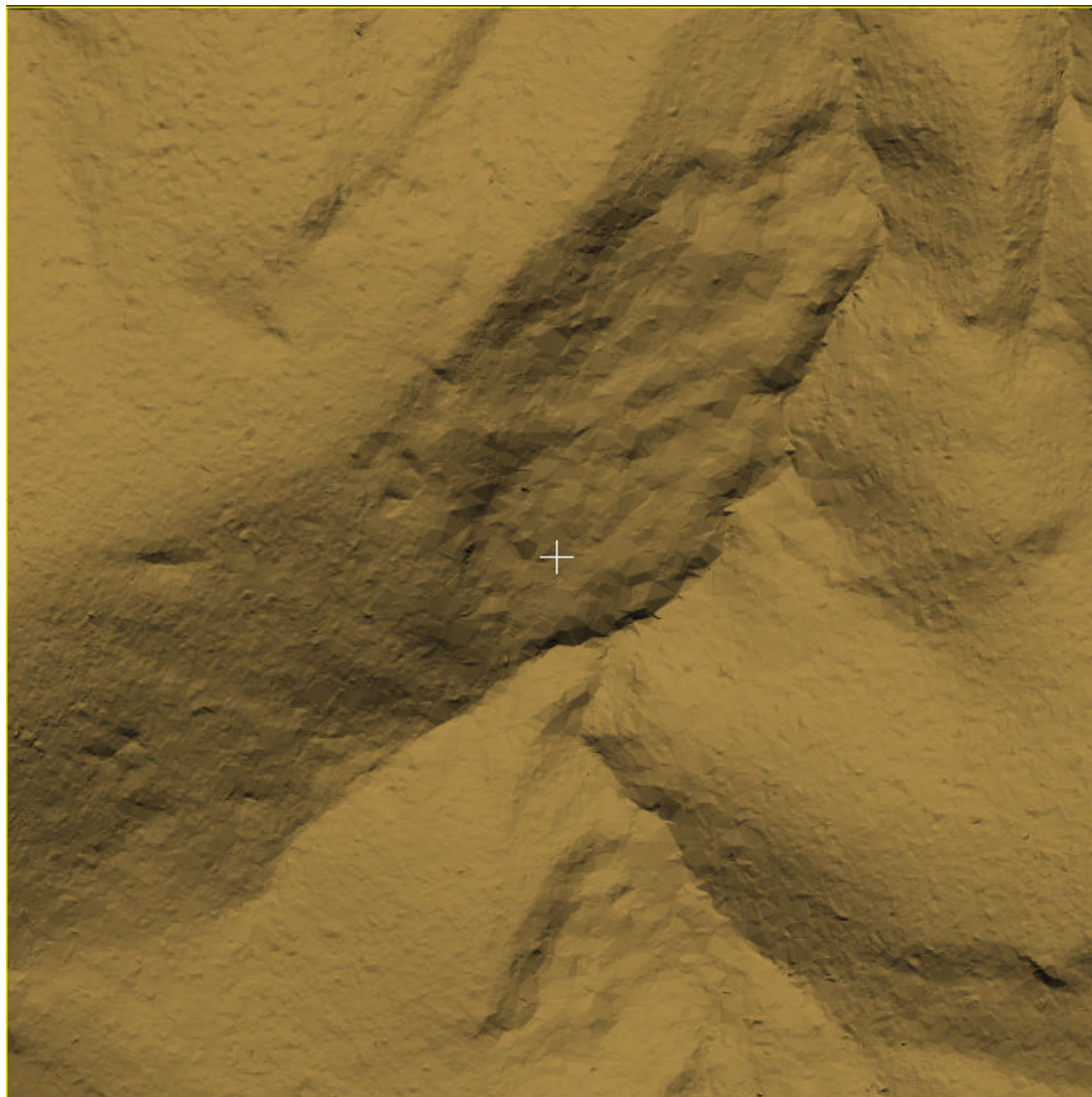
TRIAL D

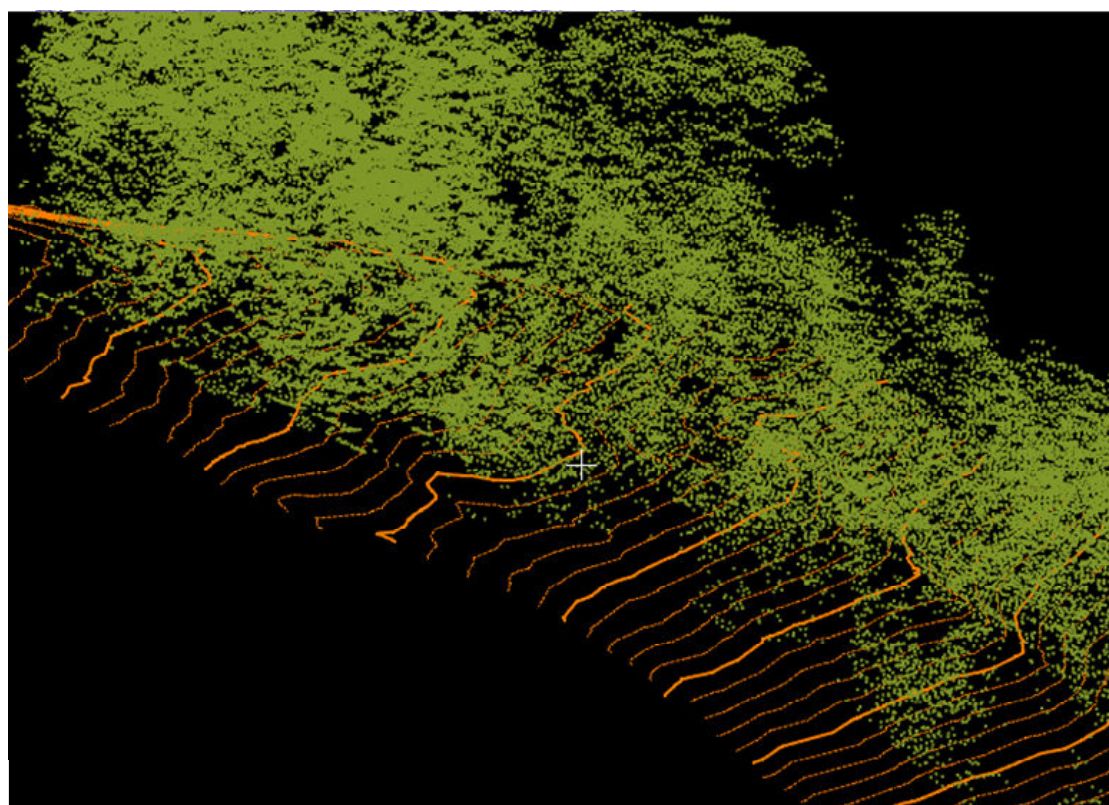
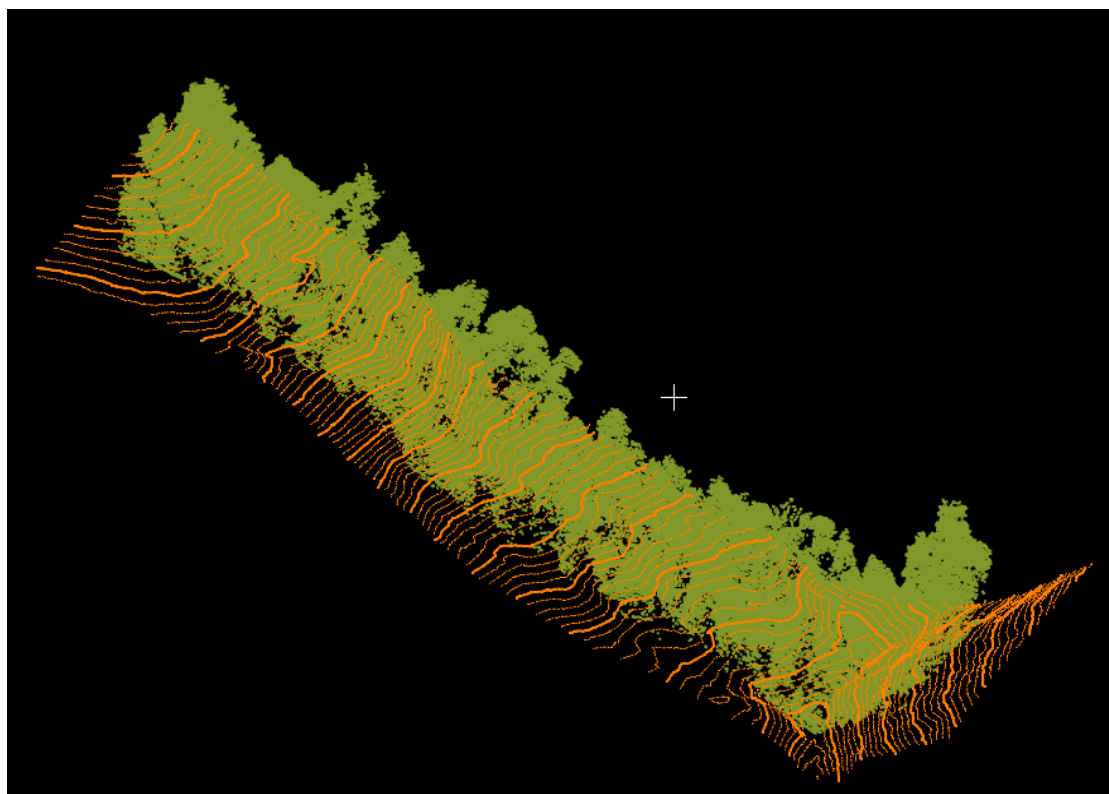


FORESTRY TASMANIA

TYPICAL TILE – LAS FORMAT

Largest tile 7.3 million points 200MB - Trial A Tile e3660n54135.las



TYPICAL CROSS SECTIONS (1m contours and vegetation shown)

Appendix 5: Spline interpolation

Experience gained in processing LiDAR data from northeast Tasmania (Green and Bombardieri, 2013) was built upon for the Luina project. A 100 m² area was chosen and various interpolation methods tested. As in northeast Tasmania, a thin plate spline method was found to produce hillshade images that best highlighted bedding features.

Experiments were undertaken by Robert Musk of Forestry Tasmania using algorithms written in the R language. He measured the relative improvements gained by modifying two spline parameters: lambda and the search method.

For each ground point the fitted spline used in standard interpolation is subject to a variously termed smoothing, tension or roughness parameter lambda. If lambda is high, the spline will be very smooth and if it is very small, the spline will very closely model all ground points, but be subject to “over-fitting”, where noise can reduce the value of the result (Fig. A5.1). An optimal lambda that minimises residual sum of squares (RSS) was calculated by generalised cross-validation (GCV) (e.g., Fig. A5.2) and then incrementally reduced in an attempt to increase subtle signal (as well as noise and over-fitting).

For the Luina data it was found that reducing lambda had no effect on the definition of geological bedding, although rectangular artefacts were generated as lambda decreased (Fig. A5.3). The lack of improvement in signal and an additional observation that noise did not increase with decreasing lambda together indicate that the processing method in classifying ground points must have introduced a limit to the degree of roughness (including noise) in the classified ground point data. The survey contractor would have used spline surface interpolation as part of the process for classifying ground points, and any smoothing introduced at that point would limit the roughness of any DEM subsequently derived by spline interpolation. The experiment indicates that because the classification process introduced a roughness limit, we may use a very small lambda in fitting splines because over-fitting cannot occur. However, a minimum limit for lambda is in practice provided by that point at which artefacts are generated. In practice, reducing lambda by a factor of 10 times was possible before significant artefacts were generated.

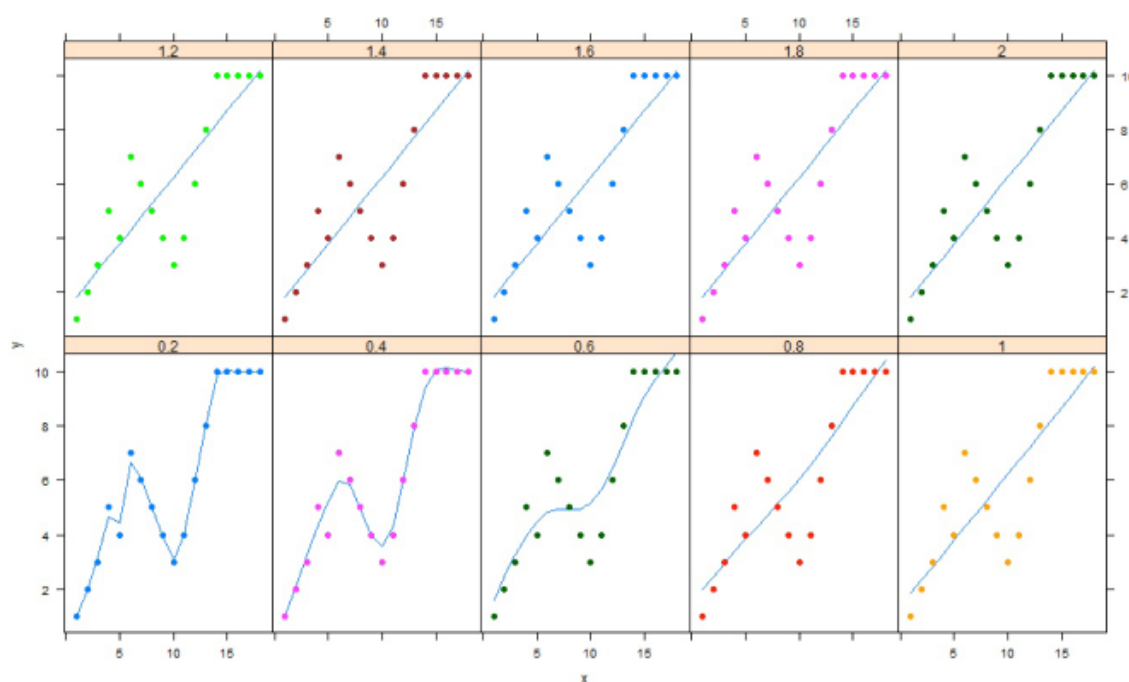


FIGURE A5.1 Spline fits for various lambda (actually the equivalent in R: spar). There is an optimum at 0.4. A lower lambda results in “over-fitting” where noise has an unwanted influence, and a larger value results in “under-fitting” that in the limit approximates linear regression. From StackOverflow (2013).

Ground points contributing to spline surfaces are typically selected based on a search radius and/or minimum number contributing (neighbouring) points. A lambda routine was produced that gathered contributing points attempting to ensure that each angular sector was equally represented. As additional contributing points were added, the spline surface increased in quality, but improvements were not noticeable beyond three added points, corresponding to about 20 neighbours used for each grid point (Fig. A5.3). It

is concluded that standard algorithms for searching for neighbouring points suffices to produce an adequate interpolation.

Based on the results of these experiments, the Luina data was interpolated using spline interpolation with low lambda: the Minimum Curvature surface interpolation tool in Encom's MapInfo Discover software, with Tension = 0. The software logs are provided in Appendix 6.

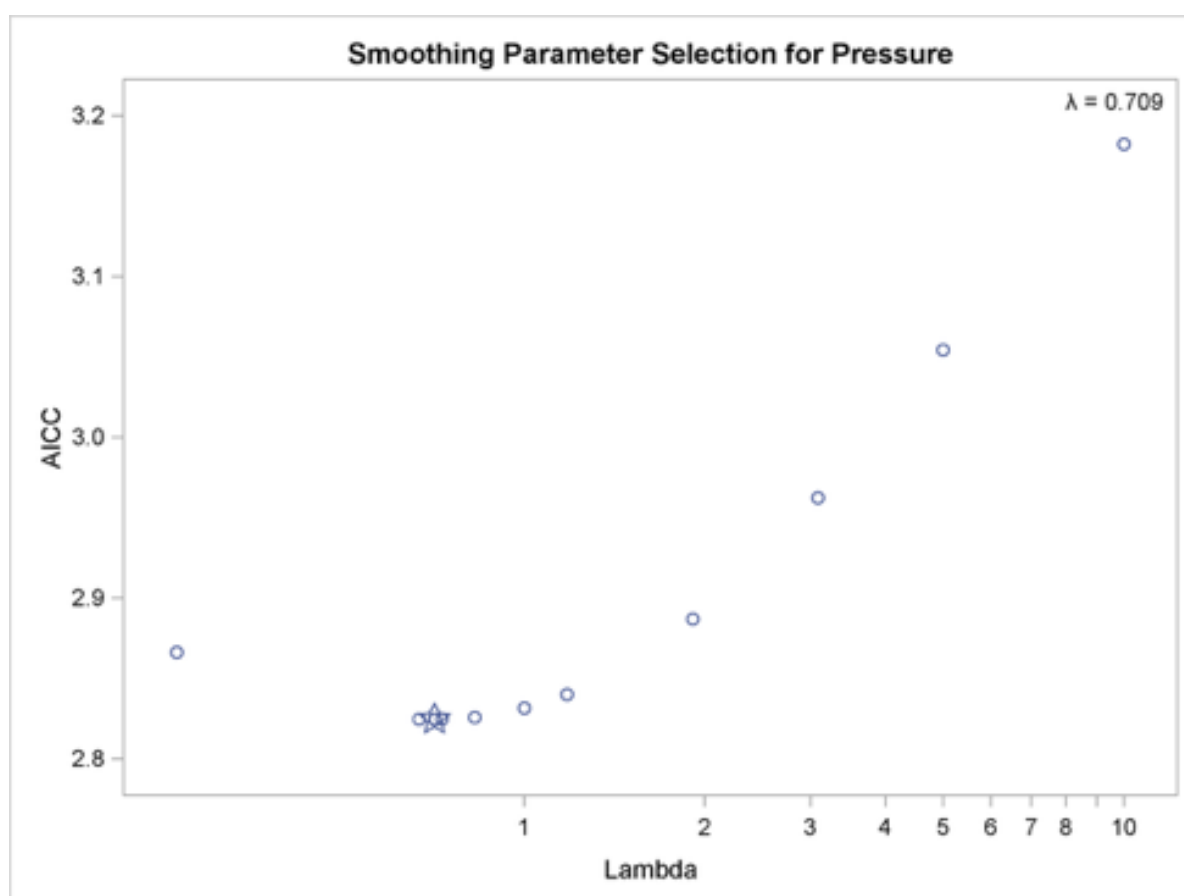
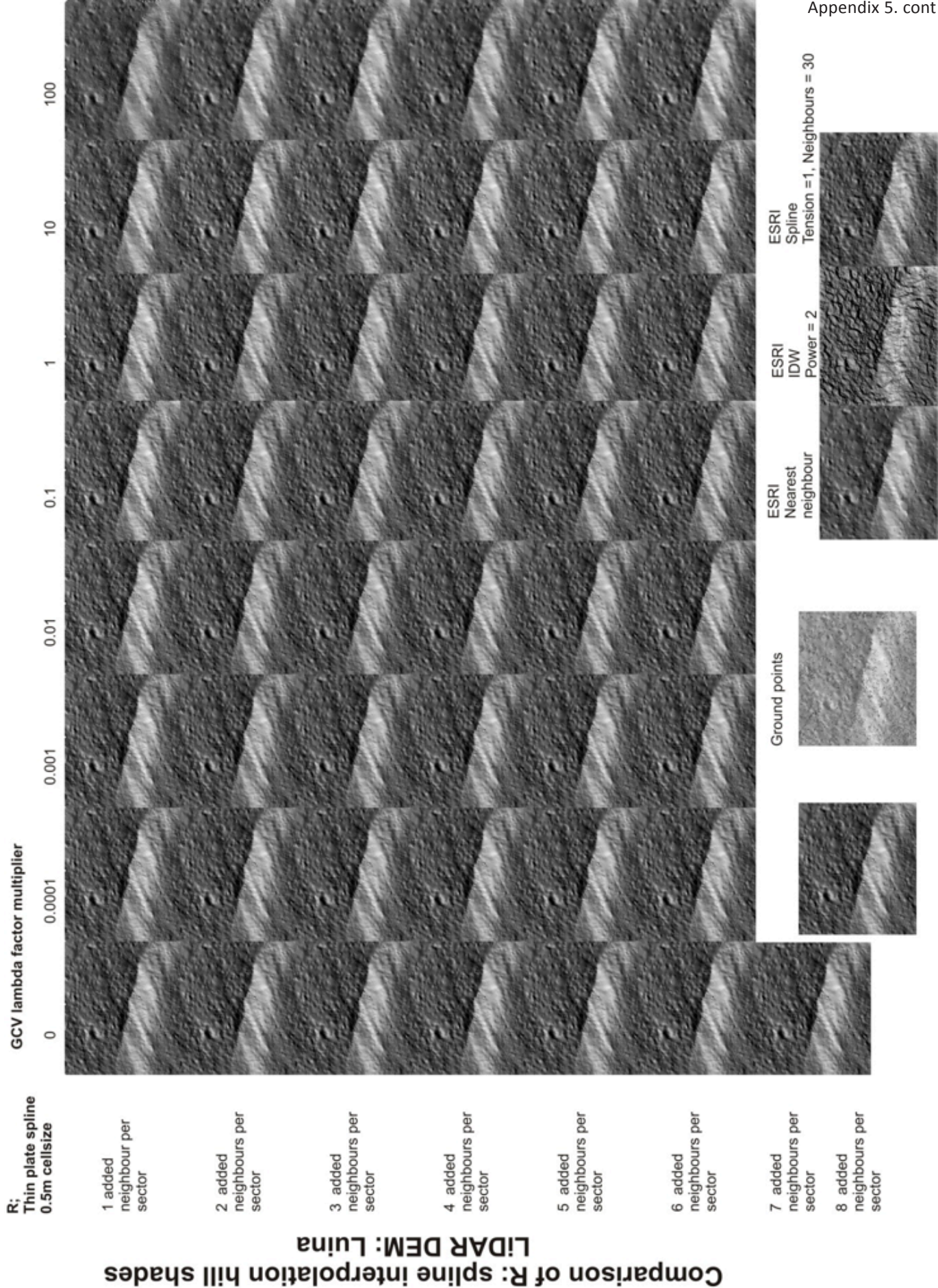


FIGURE A5.2 A fitting criterion (in this case the Akaike Corrected-Information Criterion rather than the typical Residual Sum of Squares GCV) is calculated as a function of lambda illustrating the typical result that lambda has a minimum (indicated with a star symbol). The usually accepted optimal lambda lies between under-fitting (high values of lambda) and over-fitting (low values of lambda). From SAS (2014).

FIGURE A5.3 (Opposite page) A collation of hillshaded DEMs resulting from various interpolation techniques and parameters. The thin plate spline method produces images that best highlight bedding features. The images demonstrate that reducing lambda (by decreasing the GCV lambda factor multiplier) increases the definition of geological bedding up to a point (at ~0.1), beyond which there is no improvement, or artefacts are generated. Increasing the number of contributing ground points (neighbours) by up to 3 per sector (see text) improves the DEM, but additional sampling provides no further improvement. The test area of 300 m x 200 m is centred on 365740mE, 5419253mN (GDA94).



Appendix 5. cont

REFERENCES

- SAS 2014. *SAS/STAT(R) Users Guide*. Viewed at http://support.sas.com/documentation/cdl/en/statug/63347/HTML/default/statug_transreg_sect060.htm
- STACKOVERFLOW 2013. *How do I select the smoothing parameter for smooth.spline?*. Viewed at <http://stackoverflow.com/questions/14929268/how-do-i-select-the-smoothing-parameter-for-smooth-spline>

Appendix 6: DEM interpolation processing logs

Surface interpolation from LiDAR ground points was calculated using Encom's MapInfo Discover software. The Minimum Curvature batch processing tool directly read .las files as provided by the survey contractor. Default parameters were used except for Tension = 0.

Logged processing instructions:

```
// General
Method = Minimum_Curvature
TotalCache = AUTO
TempDirectory = "X:\tmp\"
CoordinateSystem = "CoordSys Earth Projection 8, 116,"m", 147, 0, 0.9996, 500000, 10000000"

// Input
BandCount = 1
InputFile = LAS,"D:\Edited-Las-OptA-Class2\2Opt_A_e3630n54090.las","xyz0-----",0,0,0,0,"*.*",-1
InputFile = "D:\Edited-Las-OptA-Class2\2Opt_A_e3630n54095.las"
InputFile = "D:\Edited-Las-OptA-Class2\2Opt_A_e3630n54100.las"
InputFile = "D:\Edited-Las-OptA-Class2\2Opt_A_e3630n54105.las"
... (another 395 .las files)
InputFile = "D:\Edited-Las-OptA-Class2\2Opt_A_e3715n54195.las"

// Input coordinate data conditioning
CoordinateCondition Begin
    Null = -1e+032
CoordinateCondition End

// Input band data conditioning
BandCondition Begin
    Value2Null = 1
    Range2Null = 3,10
BandCondition End

// Input flag data conditioning
FlagCondition Begin
    Null = -1e+032
FlagCondition End

// Output
OutputFile = "X:\MRT\LIDAR\Luina2013\ERM\LuinaMinCurvFullCls2_1m.ers"
GridFormat = ERMapper
Datatype = Auto
OutputTransform = 1,0,1
GridCoordSysInfo = 0
ForceBIL = FALSE

// Data extents
DetermineExtent = YES
ParseExtentsStep = COMPLETE
CoordinateExtentMin = 363000,5408078.25
CoordinateExtentMax = 371999.99,5419999.99
BandExtentMin = 276.92
BandExtentMax = 885.41
InputStations = 54806394
ValidInputStations = 54806394
```

Appendix 6. cont

DataDensityMedian = 0.5284576416
DataDensityMax = 0.9999847412

// Grid extents
DetermineGridExtent = YES
DetermineGridCellSize = NO
GridOrigin = 362984,5408062
GridSize = 9032,11954
GridCellSize = 1,1

// Triangulation
RejectLongTriangle = 0.5
TrianglePatchMultiplier = 1

// Minimum curvature
UpwardInterpolationMethod = 1
DownwardInterpolationMethod = 1
FocusMask = TRUE
Tension = 0
DirectionBias = 1
FixedDistance = 0.01,0.01
Iterations = Normal
PercentChange = 0.00025

// Minimum curvature - stamping
StampMethod = 2
IDWRadius = 1
IDWRange = 0.25

// Minimum curvature - clipping
ClipMethod = 2
ClipNear = 4
ClipFar = 16
NearMethod = 1
FarMethod = 0

// Stamped inverse distance
SID_WorkingType = IEEE4ByteReal
SID_Radius = 4,4
SID_Model = Gaussian,250
SID_Taper = Off

// Stamped data density
SDY_Kernel = Count
SDY_Normalise = On
SDY_BiasByInput = Off

// Grid Padding
GPD_ExpandMethod = Cells,256,256
GPD_Offset = Enabled
GPD_Border = Enabled
GPD_SourceWindow = 0,0,1,1
GPD_RestoreNull = TRUE
GPD_RestoreOffset = TRUE
GPD_SourceMaskFile = ""

Processing log:

Gridding method : Minimum curvature

Input stream : 398 sources connected , total of 1534669432 bytes (indicative) Output grid band count : 1 Band 1 :

"Elevation" Type = IEEE4ByteReal

Reading : D:\Edited-Las-OptA-Class2\2Opt_A_e3630n54090.las

Warning : Data distribution may be clustered or skewed. Cell size recommendation may be poor. Coordinates are :

UTM Data separation : 1 units Data direction : 90 degrees Grid cell size recommendation : 0.25 units

Parsing input extents...

Reading : D:\Edited-Las-OptA-Class2\2Opt_A_e3630n54090.las Reading : D:\Edited-Las-OptA-Class2\2Opt_A_e3630n54095.las ... (Another 395 .las files)

Reading : D:\Edited-Las-OptA-Class2\2Opt_A_e3715n54195.las Parse input extents : Elapsed time 171 s Total input points : 54806394 Total valid input points : 54806394 Spatial range X : (363000 to 371999.99) 8999.99 Spatial range Y : (5408078.25 to 5419999.99) 11921.74 Point separation : <=0.5 (Avg : 0.436537364) : 17086178 stations Point separation : <=1 (Avg : 0.844540726) : 5839013 stations Point separation : <=2 (Avg : 1.521892926) : 6003411 stations Point separation : <=4 (Avg : 2.913529212) : 6294957 stations Point separation : <=8 (Avg : 5.818442463) : 7002730 stations Point separation : <=16 (Avg : 11.41040823) : 7079963 stations Point separation : <=32 (Avg : 21.89154432) : 4226316 stations Point separation : <=64 (Avg : 41.40664117) : 1117210 stations Point separation : <=128 (Avg : 78.05323641) : 98244 stations Point separation : <=256 (Avg : 155.6088927) : 2687 stations Point separation : <=512 (Avg : 417.2202435) : 1512 stations Point separation : >512 (Avg : 590.6576924) : 454 stations Band 0 range : 276.92 to 885.41 Data coverage : Number of tiles 1 occupying area 6.871947674e+010 Data coverage : Number of cells 1590 occupying area 104202240 Data coverage : Minimum density 0.003265380859 points/unit area (Square of length 17.49979973 units) Data coverage : Maximum density 0.9999847412 points/unit area (Square of length 1.000007629 units) Data coverage : Mean density 0.5242352372 points/unit area (Square of length 1.381137431 units) Data coverage : Median density 0.5284576416 points/unit area (Square of length 1.375608684 units) Data coverage : Mode density 0.9999847412 points/unit area (Square of length 1.000007629 units) Grid size : (9032 x 11954) cells of size (1,1) Grid extent : (362984 5408062) to (372016 5420016) Patch coverage : 153 patches of size 1128 x 746 cells with 358211 points per patch. Patch coverage : 153 patches occupied (estimated) with 358211 points per patch.

Source data stamping will be performed direct to memory.

Source data will be in virtual memory. Patch cache size : 16 bytes

Prepare gridding : Elapsed time 1 s

Sorting input data...

Reading : D:\Edited-Las-OptA-Class2\2Opt_A_e3630n54090.las Reading : D:\Edited-Las-OptA-Class2\2Opt_A_e3630n54095.las ... (Another 395 .las files)

Reading : D:\Edited-Las-OptA-Class2\2Opt_A_e3715n54195.las Sort input data : Elapsed time 2141 s Patch statistics : 130 occupied patches Patch statistics : Maximum points 733972, minimum 928 Patch statistics : Median points 443166

Stamping input data... Stamped a total of 30708419 grid cells : 28.44200951 percent Stamp input data : Elapsed time 247 s

Interpolation phase 1...1:2:3:4:5:6:7:8:9:10:11:12:13:14: Interpolation phase 1 : Elapsed time 3 s

Creating clip mask... Create clip mask : Elapsed time 34 s

Focus source mask...

Interpolation phase 2... Interpolation phase 2 (13): Interpolation phase 2 (12): Interpolation phase 2 (11):

Interpolation phase 2 (10): Interpolation phase 2 (9): 0 Interpolation phase 2 (8): 0 Interpolation phase 2 (7): 0

Interpolation phase 2 (6): ++++ Interpolation phase 2 (5): +++0 Interpolation phase 2 (4): +0 Interpolation phase 2 (3):

0 Interpolation phase 2 (2): 0 Interpolation phase 2 (1): 0 Interpolation phase 2 (0): 0 Interpolation phase 2 : Elapsed time 20 s

Interpolation phase 3...0

Interpolation phase 3 : Elapsed time 61 s

Exporting grid...

Writing grid header...

Output header : X:\MRT\LIDAR\Luina2013\ERM\LuinaMinCurvFullCls2_1m.ers

Writing grid data...

Write grid data : Elapsed time 17 s

Appendix 6. cont

Output grid data : X:\MRT\LIDAR\Luina2013\ERM\LuinaMinCurvFullCls2_1mWriting TAB companion... Output TAB
companion : X:\MRT\LIDAR\Luina2013\ERM\LuinaMinCurvFullCls2_1m.tab Export grid : Elapsed time 18 s
Releasing memory and erasing temporary files...
Gridding complete : Elapsed time 2702 s

Appendix 7: MOI tools

Matt Cracknell (Polyspectral Services) was contracted to deliver an interactive tool in the ArcMap environment to extract bedding orientations from digitised curvilinear DEM features. The work built on Cracknell's BSc(Hons) study in which he used the moment of inertia (MOI) method to estimate 1200 bedding orientations from a LiDAR DEM (Cracknell 2009).

A tutorial on the MOI tool is reproduced in full below and all digital files are attached to this report.

The MOI tool was used to assist interpretation of the Luina LiDAR DEM. The tool proved to be practical for deriving reconnaissance structural measurements. The experience also resulted in the development of constructive notes useful in implementing the tool:

Tips and tricks

- You'll need either the ArcGIS Spatial Analyst or 3D Analyst extension (via Customise – Extensions ...)
- Don't try to digitise a line comprising just 2 points – you'll get an error.
- Just before running MOI_V2, delete the M-K graph (otherwise they build up in the taskbar).
- Points with high M and low K (i.e. the best Geolines) can plot off the graph.

Handy procedures

- Replace MOI_scratch.gdb INPUT_DEM with desired DEM

Rename INPUT_DEM to INPUT_DEM_testdata

Open Arc Catalog. Right click on MOI_scratch.gdb and select Import – Raster datasets

Change name to INPUT_DEM

Add the DEM to the project.

This is also a good place to put all the imagery you'll use.

- Manually create GeoPoint layer coloured by K-M Quality
<1 is bad (blue), >1 is good (red)

Copy GeoPoint

Paste as new layer (the old layer gets deleted every time you run MOI)

Rename to GeoPoint pt

Open Attribute table

Add Field: Quality, double

Right click on Quality field header and select Field calculator

Tick Show codeblock

Paste into VB Script codeblock:

If [K] > (-0.1 * [M] + 1.2) Then

 Q = 0.8 / [K]

Else

 Q = [M] / 4

End If

Add Quality = Q

Edit symbology – Import GeoPoint pt.lyr (<1 blue, 1 yellow-green, >1 red)

REFERENCE

CRACKNELL, M. J. 2009. Remote sensing geological structures using high resolution Digital Elevation Models. B.Sc. Honours thesis, University of Tasmania, Hobart, Tasmania.



M. Cracknell

July 2014

Polyspectral Services

polyspectral.services@gmail.com

MOI Toolbox – Version 2

Summary

This document provides a tutorial on the use of the MOI ArcGIS toolbox. The MOI toolbox provides a set of models to semi-automate the process of generating geological feature (e.g. bedding) dip and dip direction measurements from a high resolution Digital Elevation Model (DEM). Dip and dip direction measurements are estimated using the Moment of Inertia (MOI) algorithm (Fernández, O. 2005). The MOI algorithm requires a set of 3D points (X, Y and Z) to estimate, based on matrix algebra, the orientation of a plane that best-fits these 3D points. In addition to estimating the orientation of a plane, the MOI algorithm also provides an indication of the reliability of the fit of the plane with respect to the 3D points. These reliability metrics symbolise the distribution of the 3D points around the estimated plane (M) and the colinearity/coplanarity of the 3D points (K).

Extensive experimentation has indicated that curvature (profile, plan and average) DEM derivatives provide an optimal visualisation environment for the identification of small-scale (10-100 m) topographic features that represent the surface expression of geological features (bedding planes). High (and low) DEM curvature is used as a guide for digitising a set of vertices which are then converted into 3D geolocated points. It is from these 3D points that the MOI algorithm estimates best-fit plane orientation. Detailed information on the theory and practical considerations of this workflow can be found in Cracknell (2009) and Cracknell *et al.* (2013).

Software requirements and files

The MOI Toolbox was developed on a Microsoft Windows 64-bit operating system and uses a combination of ArcGIS 10.0 tools and Python 2.6 (32-bit) scripts. Testing with other versions of these applications has not been conducted although it is likely that later versions will work. The MOI script requires several modules which are supplied with the accompanying files (see below). ArcGIS current (MOI_template.gdb) and scratch (MOI_scratch.gdb) workspaces contain template and intermediate spatial data files in Projected Coordinate System GDA 1994.

The following files are provided in the MOI directory:

MOI

- Python_modules (contains the Python 2.6 (32-bit) modules that must be installed)
 - matplotlib-1.3.1.win32-py2.6

- numpy-1.8.1-win32-superpack-python2.6
 - pyparsing-2.0.2.win32-py2.6
 - python-dateutil-2.2.win32-py2.6
 - scipy-0.14.0-win32-superpack-python2.6
 - six-1.6.1.win32-py2.6
- MOI_template.gdb (ArcGIS current workspace)
- GeoLines (polyline feature class)
 - GeoPoint (point feature class)
 - points3D (polyline vertices feature class)
 - MOI (toolbox)
 - ♦ DEM curvature (model to generate and display DEM derivatives)
 - ♦ MOI.py (link to MOI Python script)
 - ♦ MOI_V2 (model to generate 3D plane and display its properties)
- MOI_scratch.gdb (ArcGIS scratch workspace)
- DEM
 - Various files generated by the MOI Toolbox
- references (reference documents)
- Cracknell_2009.pdf (reference document)
 - Cracknell_etal_2013.pdf (reference document)
- GeoPoint.lyr (point feature class symbology)
- MOI.png (image displaying plane properties)
- MOI_dat.csv (data file)
- MOI.py (MOI Python script)
- MOI_template.mxd (ArcMAP document)
- vector.py and vector.pyc (required Python and compiled Python files)
- MOI_Toolbox_Version2.pdf (this document)

Setup

Create a directory called ArcGIS on the C:\ drive of the computer you will be using (C:\ArcGIS\) and copy the MOI directory to this location. Install Python 2.6 modules starting with numpy, scipy and matplotlib followed by the others. Open the MOI_template.mxd using ArcMAP. If the MOI Toolbox is not available in the ArcToolbox window add the MOI Toolbox located in MOI_template.gdb. Open the MOI Toolbox and check that DEM curvature (model), MOI (script) and MOI_V2 (model) are available (Figure 1).

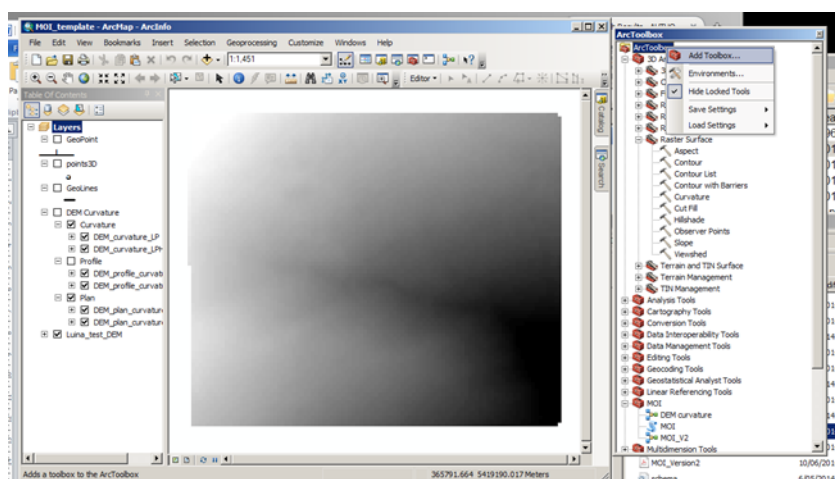


Figure 1. Screen grab showing ArcToolbox window (with MOI Toolbox installed). Add Toolbox ... if the MOI Toolbox is not visible.

Tutorial

This tutorial is based on the Luina_test_DEM raster file located in MOI_scratch.gdb. This DEM was interpolated from LiDAR ground returns with a resolution of 2 m.

1. Generating DEM curvature

The *DEM curvature* model takes a raster DEM file and calculates curvature derivatives (profile, plan and average). Profile curvature is the curvature of the surface in the direction of slope and plan curvature is the curvature of the surface perpendicular to the slope direction. Average curvature is the average of these two curvature derivatives. Curvature derivatives are then smoothed using a mean spatial filter. Displaying these layers with red-blue (high-low) colour ramp and a sun angle filter is recommended. This visualisation aids the identification of topographic features representing the surface expression of bedding planes

Open the *DEM curvature* tool and set the following parameters:

- ◆ DEM – input DEM
(for all curvature derivatives)
- ◆ Neighbourhood (defaults to rectangular 3x3) –neighbourhood for mean spatial filter

2. Digitising geological features

It is easier to visualise the surface expression of a bedding plane as high curvature features indicating resistance to weathering and erosion (e.g. indurated siliciclastic sedimentary rocks - quartzite). However, low curvature features may represent faults or features that are less resistive to weathering and erosion.

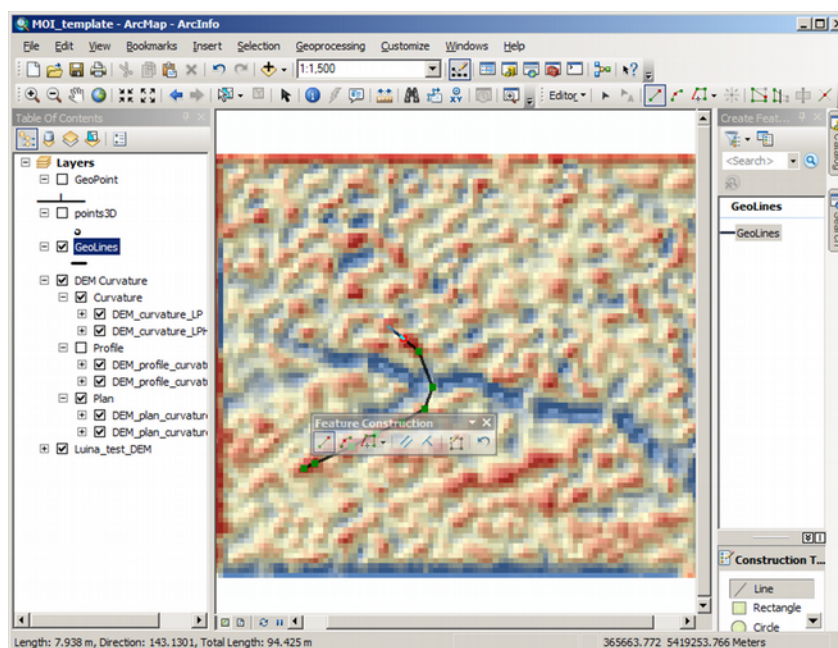


Figure 2. Digitising a GeoLines polyline feature from the DEM curvature (average) raster generated by the DEM curvature model.

Once a potential feature has been identified make the *GeoLines* feature class open for editing and delete the pre-existing line if present. Carefully place vertices in order along the feature of interest (Figure 2). Vertices can be deleted (or added) by Right-Click ☐ Delete Vertex (Add Vertex). Multiple features can be digitised. When you are finished be sure to Right-Click ☐ Finish Sketch and then Save/Stop Editing.

3. Estimating and visualising MOI best-fit planes

The *MOI_V2* model takes the polyline feature you have digitised in the previous step and appends X (Easting m), Y (Northings m) and Z (elevation m) data, fits a plane using the MOI algorithm and then displays dip and dip direction information and associated reliability measures.

Open the *MOI_V2* tool and set the following parameters:

- ◆ *GeoLines* – input line feature class
- ◆ Scratch workspace (defaults to *MOI_scratch.gdb*)
- ◆ Current workspace (defaults to *MOI_template.gdb*)
- ◆ *INPUT_DEM* – DEM used to append elevation (m) data

NOTE – the *MOI_V2* model looks for an *INPUT_DEM* raster object in the *scratch.gdb* workspace. Therefore, to change the file that this raster object represents it is necessary to import the target DEM file into the *scratch.gdb* and rename this to *INPUT_DEM* (this will require deleting the existing *INPUT_DEM* file first).

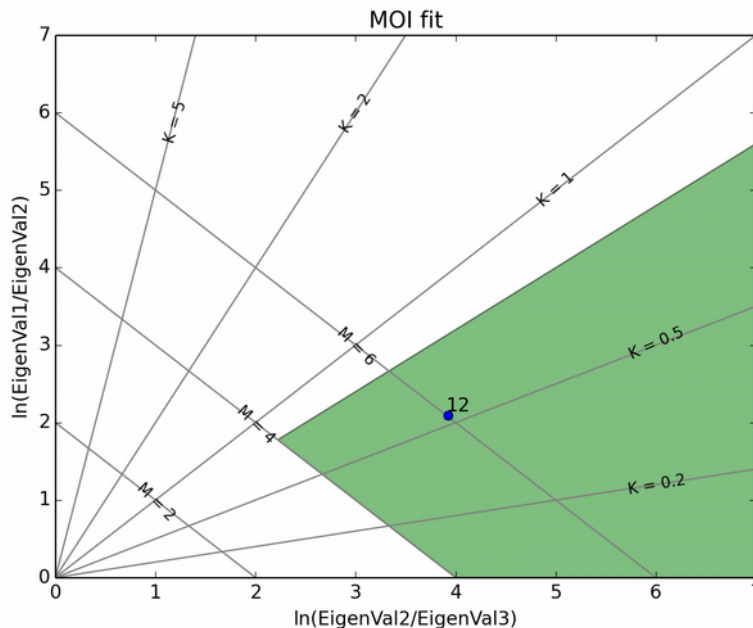


Figure 3. *MOI.png* showing the reliability of the distribution of 3D points used to estimate the best-fit plane using the MOI algorithm. High values of *M* indicate less dispersed 3D points. High values of *K* indicate increasingly colinear 3D points.

The *MOI_V2* tool should take about 1 minute to run and will work for multiple features in *GeoLines*. When *MOI_V2* has finished the ArcMAP display will have an updated set of *points3D* representing polyline vertices, *GeoPoint* plotted as dip (label) and dip direction (bedding symbol) at the midpoint of the *GeoLines* features. The *points3D* attribute table contains X, Y and Z coordinates and an Error field representing the distance from points to the MOI estimated plane. This information is useful for identifying points that are contributing to a poor fit to the MOI plane. In addition, an image will open showing a plot of the *M* and *K* reliability measures for each feature (marked with OBJECTID field) in terms of the log ratio of the three eigenvalues obtained when executing the MOI script (Figure 3). The green region indicates good *M* (≥ 4) and *K* (≤ 0.8) values. This image file is saved as *MOI.png* and will be overwritten during the next run of the *MOI_V2* model. All the information in the *GeoPoint* attribute table is written to *MOI_data.csv*. The fields in *MOI_dat.csv* are:

- **ID** = *GeoLines* feature ID
- **N_Points** = number of vertices used to generate *GeoLines* feature
- **Xmean, Ymean, Zmean** = mean X, Y and Z coordinates of *GeoLines* feature
- **M, K** = MOI reliability measures
- **RMSE** = Root mean squared error (distance) of all points to MOI estimated plane
- **A, B, C, D** = coefficients of plane
- **Dip, Dipdir** = Dip and dip direction of MOI estimated plane
- **eigen1, eigen2, eigen3** = Eigen Values of MOI estimated plane
- **Length** = Length (m) of *GeoLines* feature

These data can be loaded into other software for display and analysis. These data will be overwritten during the next run of the *MOI_V2* model.

References

CRACKNELL, M. J. 2009. Remote sensing geological structures using high resolution Digital Elevation Models. Honours Thesis (BSc.), School of Earth Sciences, University of Tasmania, Hobart, Tasmania, p. 165.

CRACKNELL, M. J., ROACH, M., GREEN, D. & LUCIEER, A. 2013. Estimating Bedding Orientation from High-Resolution Digital Elevation Models. *Geoscience and Remote Sensing, IEEE Transactions on*, vol. 51, no.5, pp. 2949-2959.

FERNÁNDEZ, O. 2005. Obtaining a best-fitting plane through 3D georeferenced data, *Journal of Structural Geology*, vol. 27, no. 5, pp. 855-858.

